ESD-TR 69-209

ESD ACCESSION LIST
ESTI Call No. 66429
Copy No. 1 of 1 cys.

ESD RECORD COPY
RETURN TO
SCIENTIFIC & TECHNICAL INFORMATION DIVISION
(ESTI), BUILDING 1211

ESD-TR-69-209
FILE COPY

AN EXPERIMENTAL INVESTIGATION OF MODIFIED DIPOLE ANTENNAS

Danai Lekhyananda

The Ohio State University
ElectroScience Laboratory
(formerly Antenna Laboratory)
Department of Electrical Engineering
Columbus, Ohio 43212

Technical Report 2648-1
2 July 1969

Massachusetts Institute of Technology
Lincoln Laboratory
Lexington, Massachusetts, 02173

AD0692783

This document has been approved for public release and sale; its distribution is unlimited.

TECHNICAL REPORT 2648-1
2 JULY 1969

AN EXPERIMENTAL INVESTIGATION OF MODIFIED DIPOLE ANTENNAS

Danai Lekhyananda

Prepared by

The Ohio State University
ElectroScience Laboratory
Department of Electrical Engineering
Columbus, Ohio

for

Massachusetts Institute of Technology
Lincoln Laboratory

Under

Purchase Order No. C-781
Prime Contract No. AF 19(628)-5167

This document has been approved for public release and sale;
its distribution is unlimited.

ACKNOWLEDGMENTS

The author wishes to express his sincere gratitude to all those persons at the ElectroScience Laboratory and Caldwell Laboratory who aided in the completion of this study. Special recognition is given to Professor Roger C. Rudduck, his advisor, for his guidance and encouragement. Particular gratitude is extended to his supervisor, Mr. Leonard L. Tsai, whose advice and suggestions were invaluable.

The material contained in this report is also used as a thesis submitted to the Department of Electrical Engineering, The Ohio State University as partial fulfillment for the degree Master of Science.

ABSTRACT

Dipole antennas with metallic shells for housing electronic equipment at the center which are called modified dipole antennas have been investigated. Measurements were made on the input admittances and far field patterns of the modified dipole antennas with cylindrical and spherical shells. The input admittances of 120° vee-antennas with spherical shells were also measured. The metallic shells were constructed in two diameters, 0.0625λ and 0.03125λ. The operating frequency used was 375 MHz.

Admittance measurements were made using a Hewlett-Packard Model 803A VHF Bridge. Input admittances were measured as a function of antenna wire length. Radiation patterns were measured in the $E_{\theta}(\theta)$ plane for various antenna wire lengths in the resonant region.

Accepted for the Air Force
Franklin C. Hudson
Chief, Lincoln Laboratory Office

CONTENTS

Chapter		Page
I	INTRODUCTION	1
II	ADMITTANCE MEASUREMENTS	4
	A. Measurement of Admittance Using an Image Plane	4
	B. Model Constructions	4
	C. Establishment of a Calibration Standard	8
	D. Measurements Using the Hewlett-Packard Model 803A VHF Bridge	9
III	RADIATION PATTERN MEASUREMENTS	27
	A. Model Constructions	27
	B. Pattern Measurement Arrangements	27
	C. Detector Circuit	31
	D. Checking the Pattern Recording Range	32
	E. Measured Results	34
IV	CONCLUSIONS	42
Appendix		
A	TRANSFORMATION OF IMPEDANCES FROM BRIDGE REFERENCE TO APERTURE PLANE USING TRANSMISSION LINE THEORY	44
B	COMPUTER PROGRAM FOR HEWLETT-PACKARD BRIDGE MEASUREMENT	47
REFERENCES		51

CHAPTER I
INTRODUCTION

The conventional dipole antenna is one of the simplest and most widely used antennas. It is usually fed at the center by a length of transmission line which then terminates in a remote transmitter or receiver. Modern techniques have reduced the size and weight of electronic equipment to such an extent so that even high power transmitters and sensitive receivers can be produced with small dimensions. With these compact and lightweight radio equipments, it is now possible to connect them directly to the feed point of the dipole antenna, thus eliminating losses including radiation from the transmission line. These miniature equipments may be contained in metallic shells of arbitrary shape which form an integral part of the dipole antenna. The presence of these metallic housing compartments obviously will have effects on dipole performance.

The purpose of this investigation is therefore to study these effects experimentally for certain regular axially symmetric geometries. The dipole antennas with metallic shells at the center, which will be called modified dipole antennas, can have applications in communication satellites or any application that needs compact, isolated, and self-contained dipole antennas.

Measurements were made on the input admittances and far field patterns of the modified dipole antennas with cylindrical and spherical

shells as shown in Fig. 1(a). The admittance of a 120° vee-antenna with spherical shell shown in Fig. 1(b) was also investigated.

The far field, $E_{\theta}(\theta)$ patterns of the modified dipole antennas were measured at various antenna wire lengths around resonance. The measured values of beamwidth and directivity are compared with the calculated values of a conventional dipole antenna of the same overall lengths.

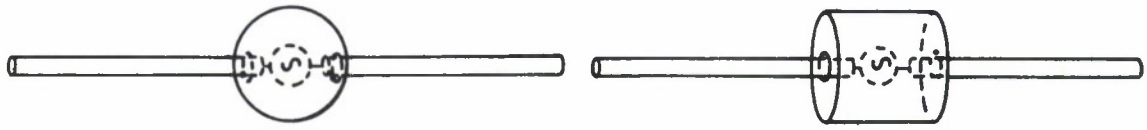

MODIFIED DIPOLE ANTENNAS WITH SPHERICAL AND CYLINDRICAL SHELLS
(a)

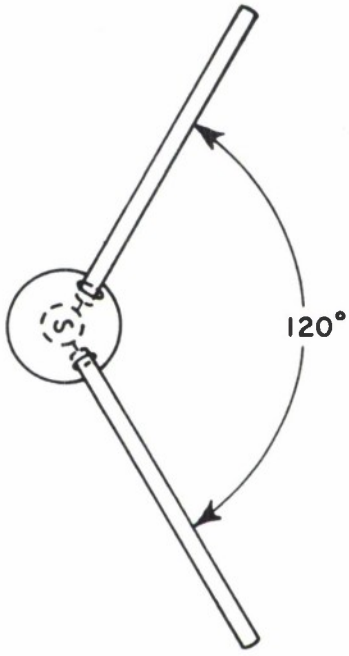

MODIFIED VEE-ANTENNA WITH SPHERICAL SHELL
(b)

Fig. 1. Modified antennas.

CHAPTER II
ADMITTANCE MEASUREMENTS

A. Measurement of Admittance Using an Image Plane

Very often when a balanced antenna such as a dipole is being investigated, it is necessary for design purposes to obtain the admittance curve of the dipole without the additional complication of a balun or parallel line feed being involved in the measurement. This may be achieved through the use of an image ground plane which then allows convenient measurements on the half dipole protruding through the ground plane with a minimum of field disturbances from peripheral equipment. The admittance of the full dipole is then simply one-half the admittance of the half dipole which is being measured.

B. Model Constructions

Since image theory is applied in the admittance measurements, only one-half of the physical antenna is needed. The spherical and cylindrical parts of the modified antennas are made of solid aluminum and are constructed in two sizes. The details of the models are shown in Fig. 2. All of the models are designed to be mounted on an aluminum ground plane and fed by a coaxial cable. The antenna-mount connector, which is also built in two sizes, connects the antenna wires by a mating screw at one end and has a type N connector at the other end, forming an integral part of the base fittings. The longer one is designed to fit on the large size group of models, and the shorter one

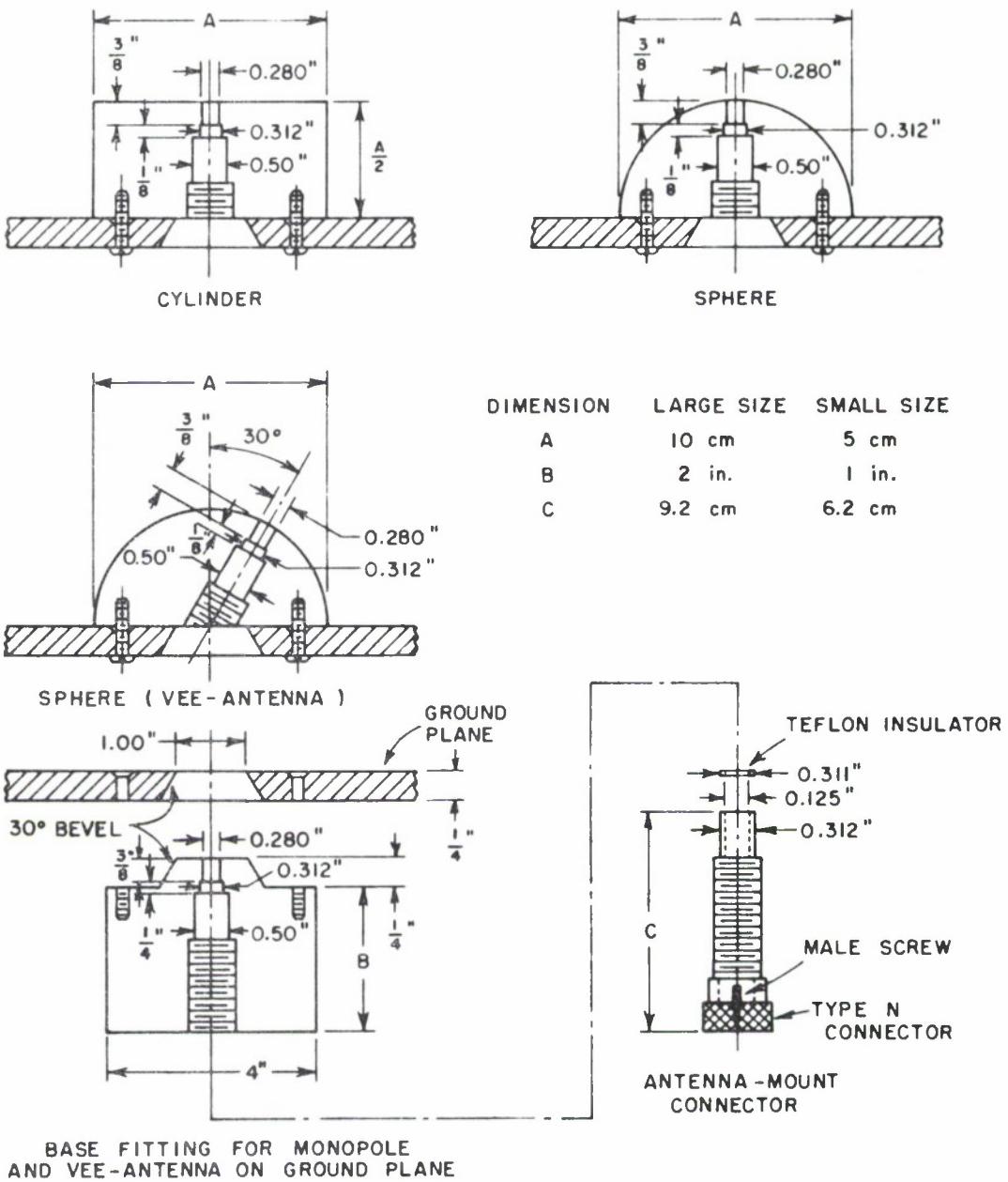

DIMENSION	LARGE SIZE	SMALL SIZE
A	10 cm	5 cm
B	2 in.	1 in.
C	9.2 cm	6.2 cm

Fig. 2. Details of model constructions for admittance measurements.

is designed to fit on the small size group of models. With such an arrangement, all the models in the large size group undergo the same condition at the feeding junction and so do all the models in the small size group.

All of the antenna models are mounted at the center of a stainless steel ground plane 0.46 m square. This ground plane is in turn mounted at the center of a large aluminum ground plane 2.46 m square mounted vertically on the outside wall of the laboratory building at a height of 5.53 m from the ground as shown in Fig. 3(a). The antenna models are shown in Figs. 3(b) to (f).

The dipole elements, hereafter called "antenna wires", are made from circular brass rod 1/8" in diameter, hence $a/\lambda \approx 0.002$. The conductivity of the rod is 10.4 Megamhos per meter as measured on a Wheatstone Bridge. Antenna wire lengths range from 10 cm to 50 cm in 2 cm increments. Smaller increments of 0.5 cm are made available through 2.5, 3 and 3.5 cm extension rods. Each rod is tapped and threaded at one end to fit the screw in the antenna-mount connector, thus providing readily interchangeable lengths of antenna wires. Short circuit reading is made available through a short piece of antenna wire attached to a circular brass cap which when inserted in the antenna-mount connector, forms a tight closure on the aperture. The measured input admittances of all geometries are referred to the apertures or the short circuit points.

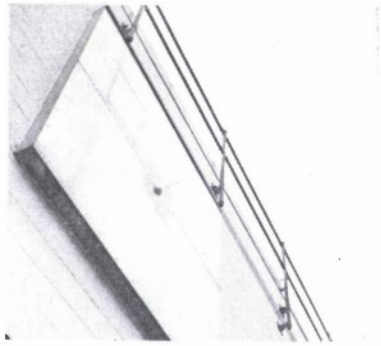

(a) GROUND PLANE ON LABORATORY WALL

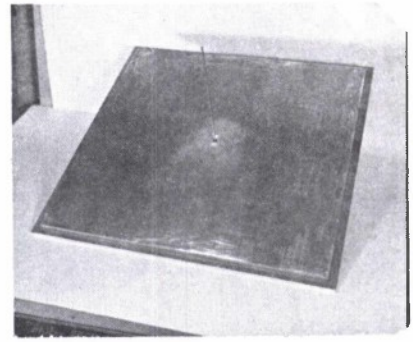

(b) MONOPOLE ANTENNA ON SMALL GROUND PLANE

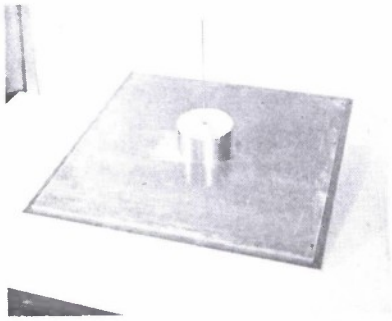

(c) MODIFIED DIPOLE ANTENNA ON LARGE CYLINDRICAL SHELL

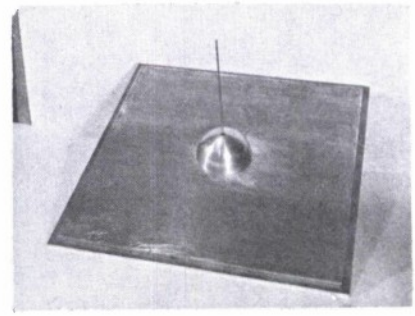

(d) MODIFIED DIPOLE ANTENNA ON LARGE SPHERICAL SHELL

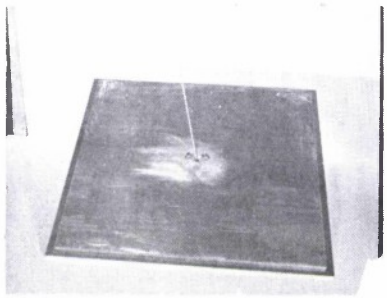

(e) UNMODIFIED VEE-ANTENNA

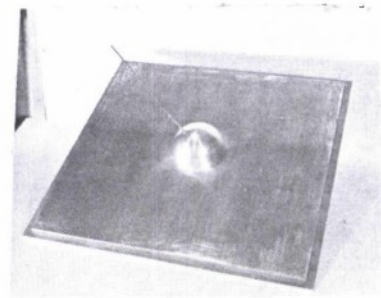

(f) MODIFIED VEE-ANTENNA ON LARGE SPHERICAL SHELL

Fig. 3. Photographs of models for admittance measurements.

C. Establishment of a Calibration Standard

The admittances obtained from each method of measurement even when corrected for the error in the equipment still shows some discrepancies from the idealized results due to the finite conductivity of the antenna wires, the finite ground plane, the finite height of antenna above ground level and the inherent errors in the setup. The possible sources of these inherent errors are discussed later and are essentially the same for each group of models because each group experiences the same environmental influences. The inherent errors can be compensated by correcting them according to the calibration curves which show the amount of deviations of the measured from the true results. In this experiment use is made of the calculated results by Otto[1] based on the Fourier Transform Method for a finite conductivity monopole antenna on a finite ground plane and a finite height above ground level as in the experiment. The measured results of the monopole antenna in our experiment, when compared to Otto's calculated results, give rise to a set of calibration curves, one for conductances and one for susceptances. Since there are two groups of models to be measured by each method, that is, large and small sizes, and each group possesses its own inherent errors, each group has its own set of calibration curves.

Also available is the calculated results by Otto for an idealized monopole antenna on an infinite ground plane.[2,3] Otto's results

are accurate since they conform very well, in fact within 0.5 millimho at the peaks, to the well known experimental results for the same case performed by Mack[4] using an accurately calibrated variable attenuator in his slotted line measurement. Otto's calculated admittance curves for both idealized and finite conductivity cases are shown in Fig. 4. The differences between both curves give an idea of how much discrepancies we can expect between calculated results, assuming infinite conductivity of antenna in free space, and practical measured results. These differences then apply to the measured results of all models.

Calculated admittances of an idealized monopole antenna on an infinite ground plane by Richmond,[5] based on the induced EMF method with ten segment solution, are also shown compared with Otto's calculated results in Fig. 4. The calculated results by both methods conform very well, and the three sets of admittance curves have the same resonant length at $h/\lambda = 0.236$.

D. Measurements Using the Hewlett-Packard Model 803A VHF Bridge

Principles of Bridge Operation[6] The model 803A operates on the Byrne-bridge principle. A schematic diagram is shown in Fig. 5. R.F. power, applied to the GENERATOR connector, is fed through a coaxial line to the impedance under measurement, connected at the UNKNOWN connector. Two probes are controlled simultaneously; one samples the E field while the other samples the H field. Each probe is connected

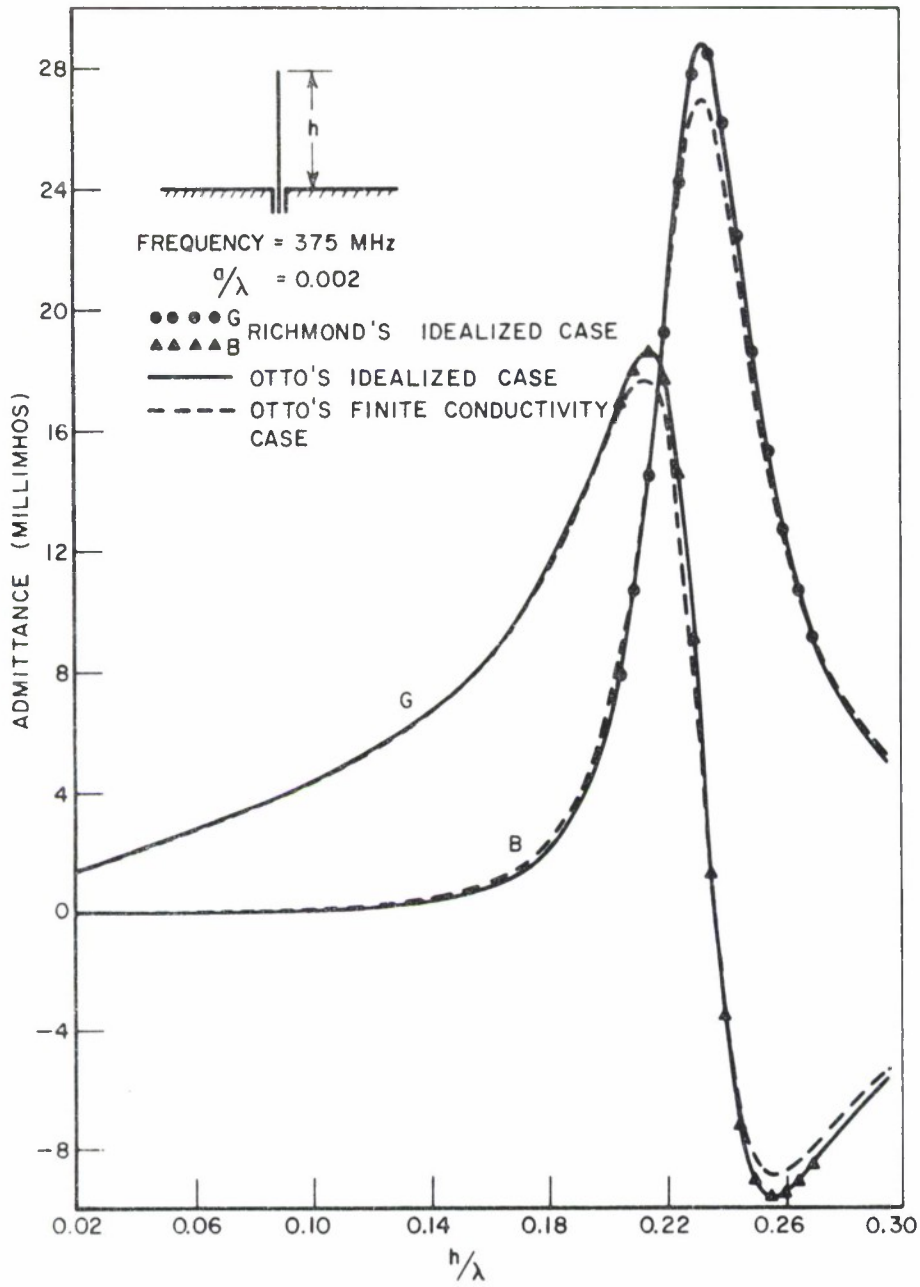

Fig. 4. Calculated admittances of a monopole antenna on ground plane by Richmond and Otto.

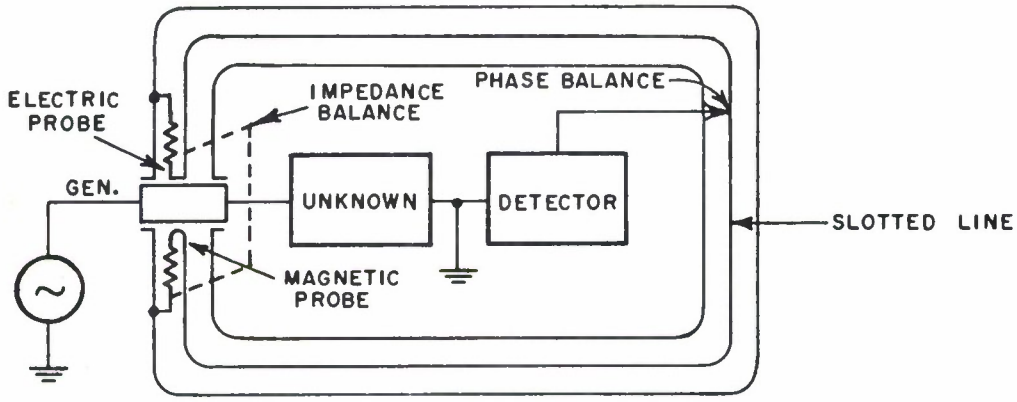

Fig. 5. Schematic diagram of Hewlett-Packard Model 803A VHF bridge.

through equal resistance to ground. The voltage developed across the resistors are applied to opposite ends of a slotted-line section. The impedance magnitude is determined by the positions the two probes have when they are adjusted so the voltages developed across their resistances are equal and therefore cancel each other at some point in the slotted line. The impedance phase angle is determined by the location of the cancellation point in the slotted line as detected by a movable probe.

The impedances obtained from the bridge dial readings are referred to a point quite close to the UNKNOWN connector on the panel.

Operation The schematic diagram of the setup for admittance measurements using the H-P model 803A is shown in Fig. 6. The antenna and the

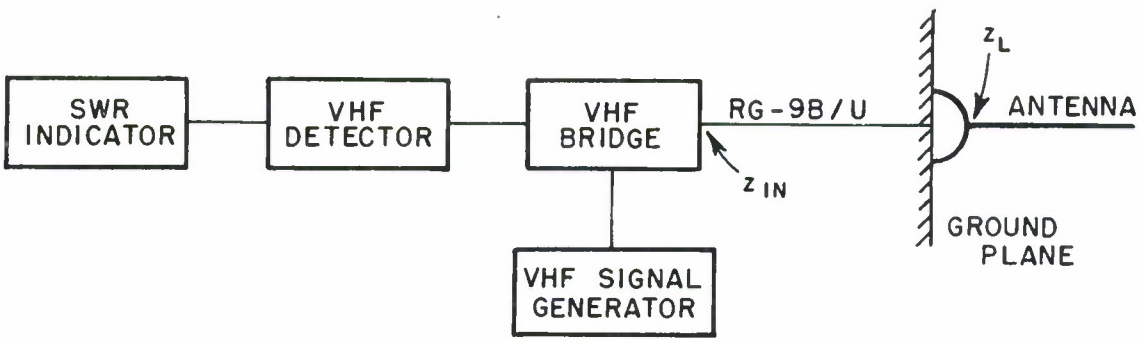

Fig. 6. Typical setup for admittance measurement by bridge method.

bridge were connected by a short length of RG-9B/U cable. The signal generator used was the Hewlett-Packard model 608C, the detector was the Hewlett-Packard model 417A and the standing-wave indicator was the Hewlett-Packard model 400C.

The 375 MHz input signal, modulated at 400 Hz was applied to the bridge. With the short circuit connected to the aperture, the bridge PHASE and MAGNITUDE controls were simultaneously adjusted to localize the null on the SWR indicator. This reading was listed as $Z_{SCM} \lfloor Z_{SCP}$ and was used as a reference for determining the amount of transformation needed to refer measured admittances to the aperture. The short circuit was then removed and the antenna wire connected in place, ready to be measured. The null and the impedance of each antenna wire length

were observed and recorded as $Z_{INM}\underline{|Z_{INP}}$.

Transformation Using Transmission Line Theory To find the impednace at the aperture, the first readings must be corrected for the impedance transformation effected by the line length between the short circuit point and the bridge by standard transmission-line equations. The admittance Y_L at the short circuit point can be calculated from the equation:

$$(1) \qquad Y_L = 20 \; \frac{1 - \dfrac{\left(1 + \dfrac{Z_{sc}}{50}\right)\left(\dfrac{Z_{in}}{50} - 1\right)}{\left(1 - \dfrac{Z_{sc}}{50}\right)\left(\dfrac{Z_{in}}{50} + 1\right)}}{1 + \dfrac{\left(1 + \dfrac{Z_{sc}}{50}\right)\left(\dfrac{Z_{in}}{50} - 1\right)}{\left(1 - \dfrac{Z_{sc}}{50}\right)\left(\dfrac{Z_{in}}{50} + 1\right)}} \quad \text{millimhos.}$$

Derivation of equation (1) is shown in Appendix A. The values of Y_L were calculated by the IBM 7094 computer where $Z_{SCM}\underline{|Z_{SCP}}$ and $Z_{INM}\underline{|Z_{INP}}$ were inputs. Z_{sc} and Z_{in} in Eq. (1) are the corrected values of $Z_{SCM}\underline{|Z_{SCP}}$ and $Z_{INM}\underline{|Z_{INP}}$ according to the correction graphs given in the bridge operating manual. The computer program is shown in Appendix B.

Measured Results The admittances of the monopole antennas on a ground plane with both large and small base fittings were carefully measured four times and the results averaged. The incremental lengths of the antenna wires were 2 cm in the off-resonant region and 0.5 cm

in the resonant region. The measured admittance curves of both cases are shown compared with the calculated results for finite conductivity case of Otto in Figs. 7 and 8. The measured curves for both cases

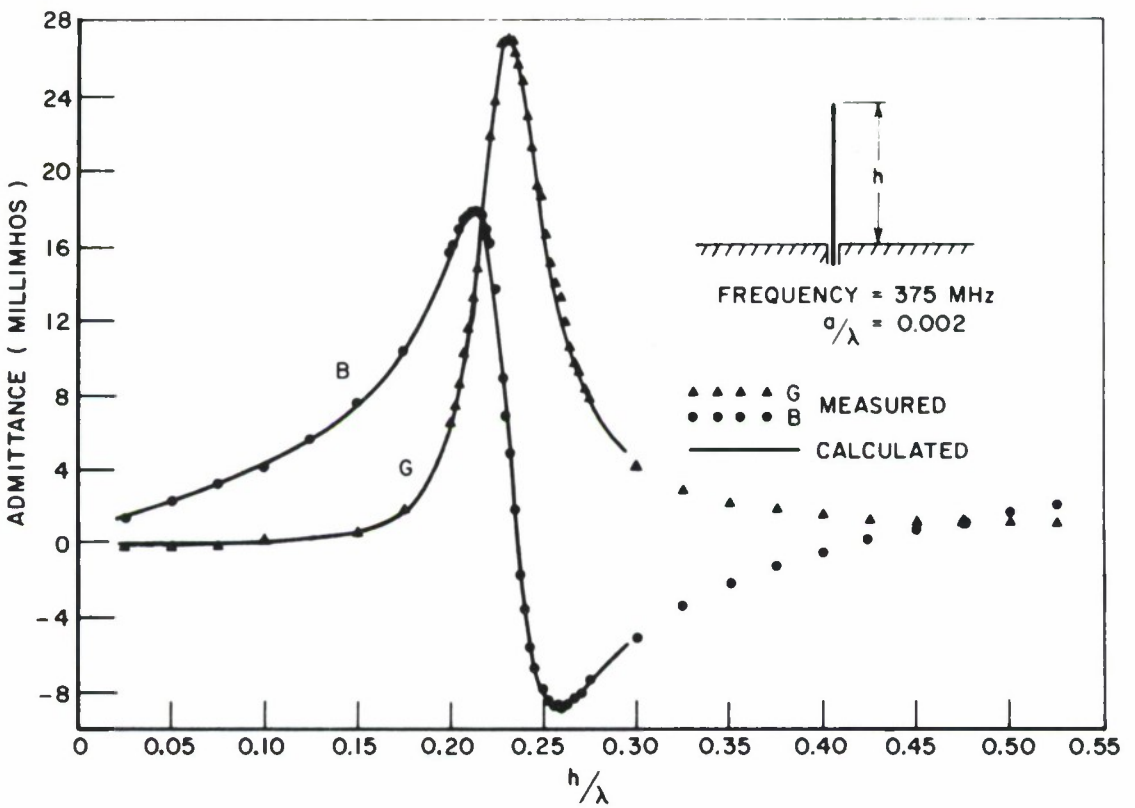

Fig. 7. Measured and calculated admittances of monopole antenna on ground plane with large base fitting. (H-P Bridge)

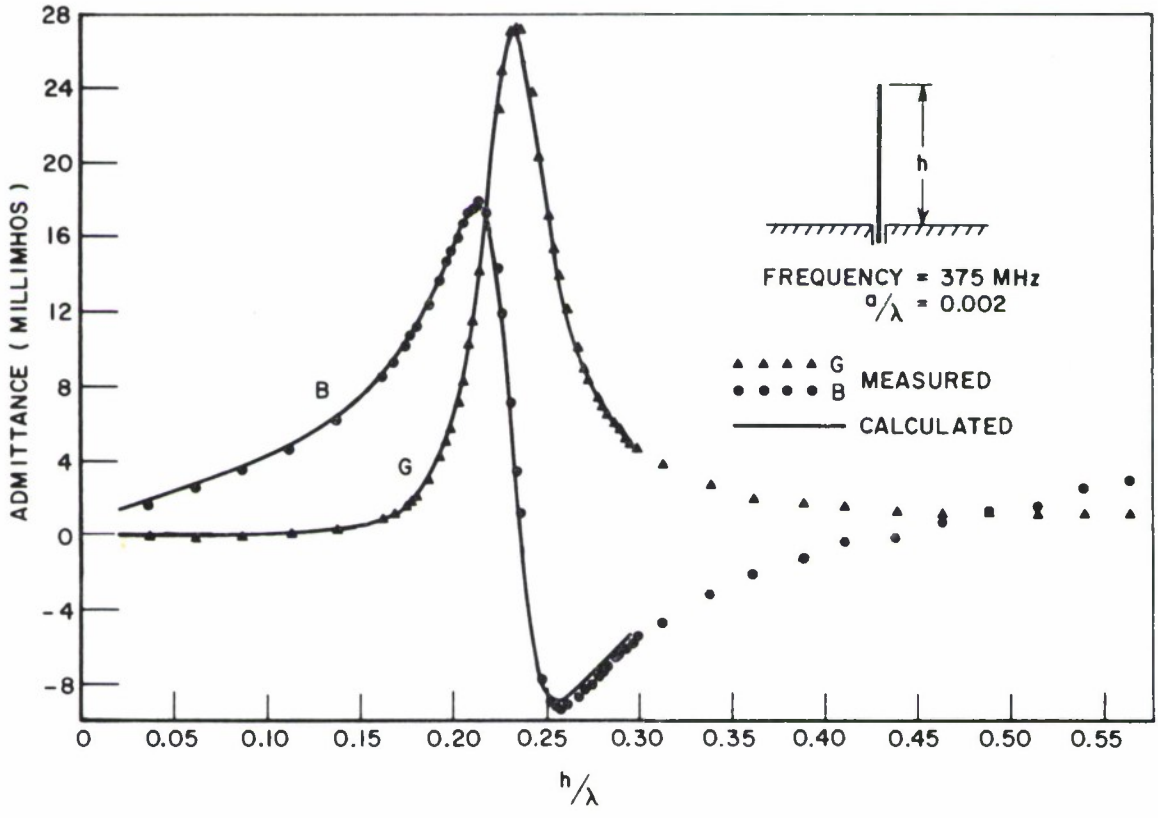

Fig. 8. Measured and calculated admittances of monopole antenna on ground plane with small base fitting. (H-P Bridge)

conform very well, within 0.5 millimho at the peaks, to the calculated curves. The resonant lengths for the measured curves of both cases occur at practically the same point as that of the calculated curves, i.e., at $h/\lambda \approx 0.236$. As a result of comparing the measured and cal-

culated results, the corresponding sets of calibration curves are obtained as shown in Figs. 9 and 10. The arrow heads on the calibration curve show the directions of increasing and decreasing susceptance values where corrections must be followed. Each set of calibration curves shows the possible amount of discrepancies of the measured values from the accurate values and applies for all models in its group.

The measured admittance curves of the modified dipole antennas on large and small cylindrical shells are shown in Figs. 11 and 12, respectively. Both cases experienced the effect of base loading and consequently the resonant lengths are shifted down practically the same amount to $h/\lambda = 0.225$. Both of the modified dipole antennas have the values of conductance and susceptance at the peaks lower than that of the unmodified dipole antenna, with the larger models having lower peaks.

The measured admittance curves of the modified dipole antennas on large and small spherical shells are shown in Figs. 13 and 14, respectively. The peak values of admittance curves of the small spherical model are almost the same as that of the small cylindrical case. However, the admittance peaks of the large spherical case are one millimho higher than that of the large cylindrical case. The resonant lengths of both spherical cases are at $h/\lambda = 0.222$ which is close to that of the cylindrical cases. It is seen that base loading of the monopole antenna by small size shells of different shapes does

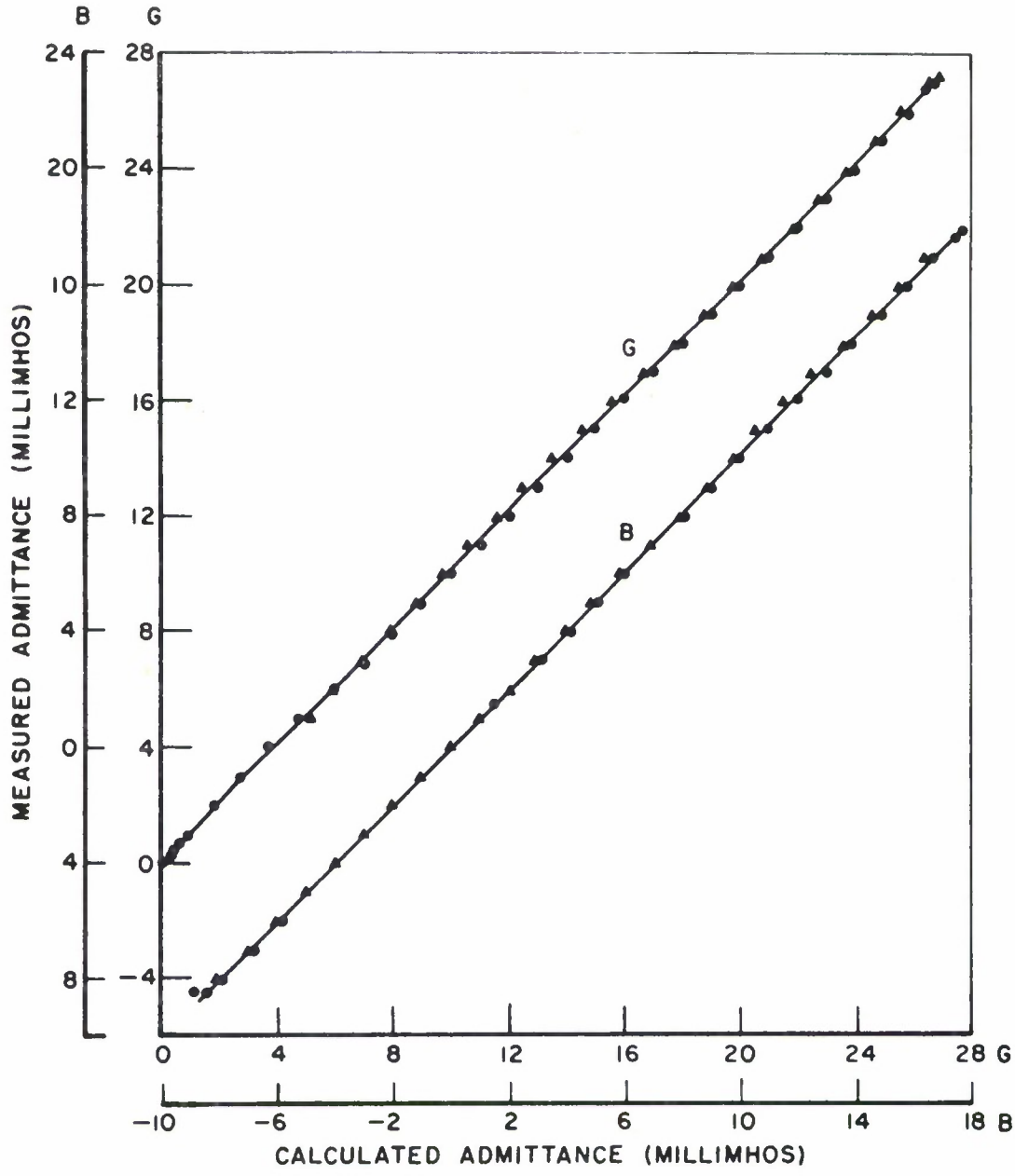

Fig. 9. Calibration curves for large size models. (H-P Bridge)

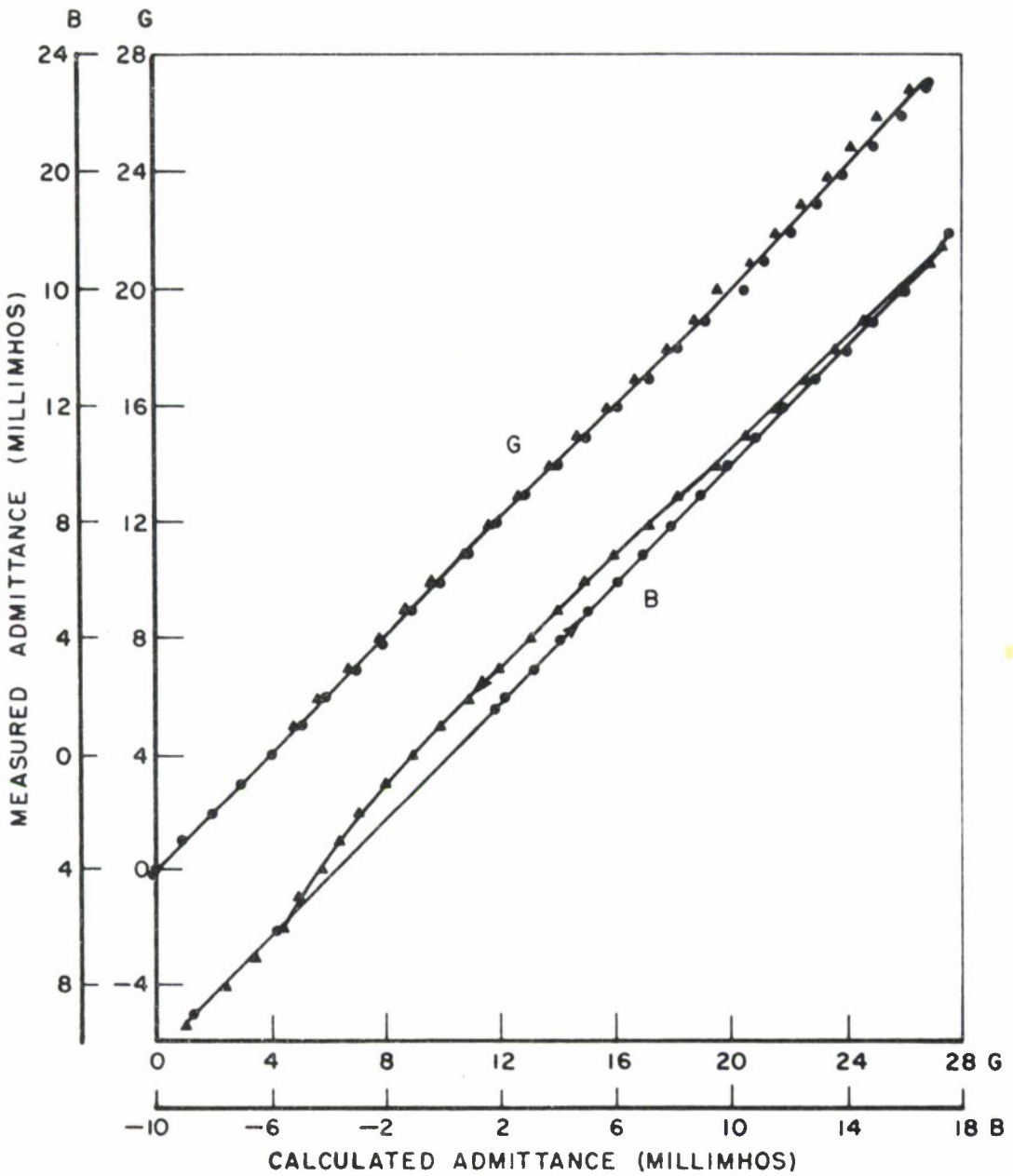

Fig. 10. Calibration curves for small size models. (H-P Bridge)

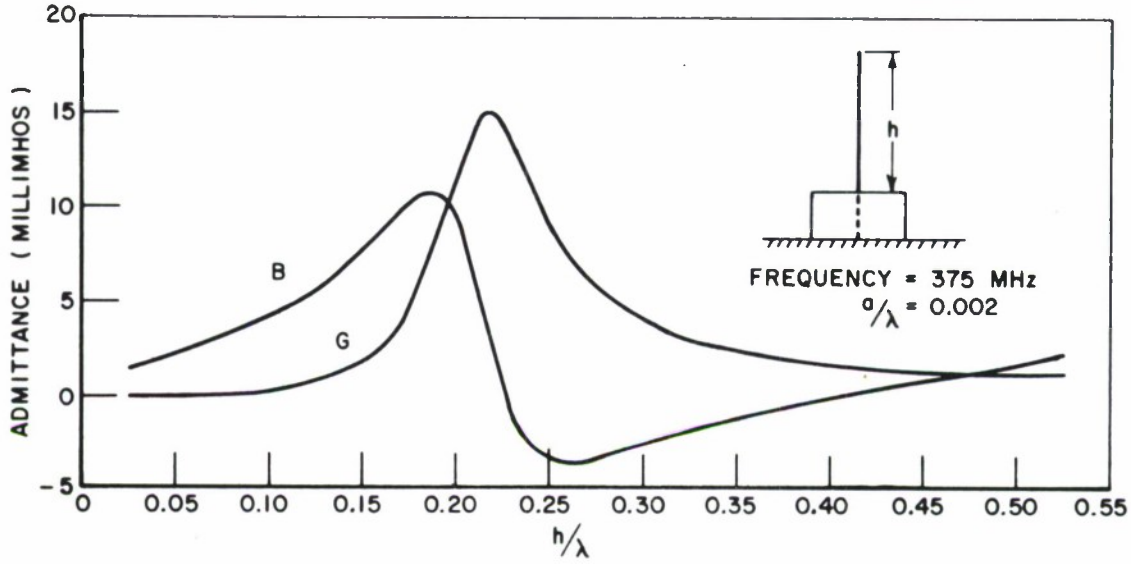

Fig. 11. Measured admittances of modified dipole antenna on large cylindrical shell. (H-P Bridge)

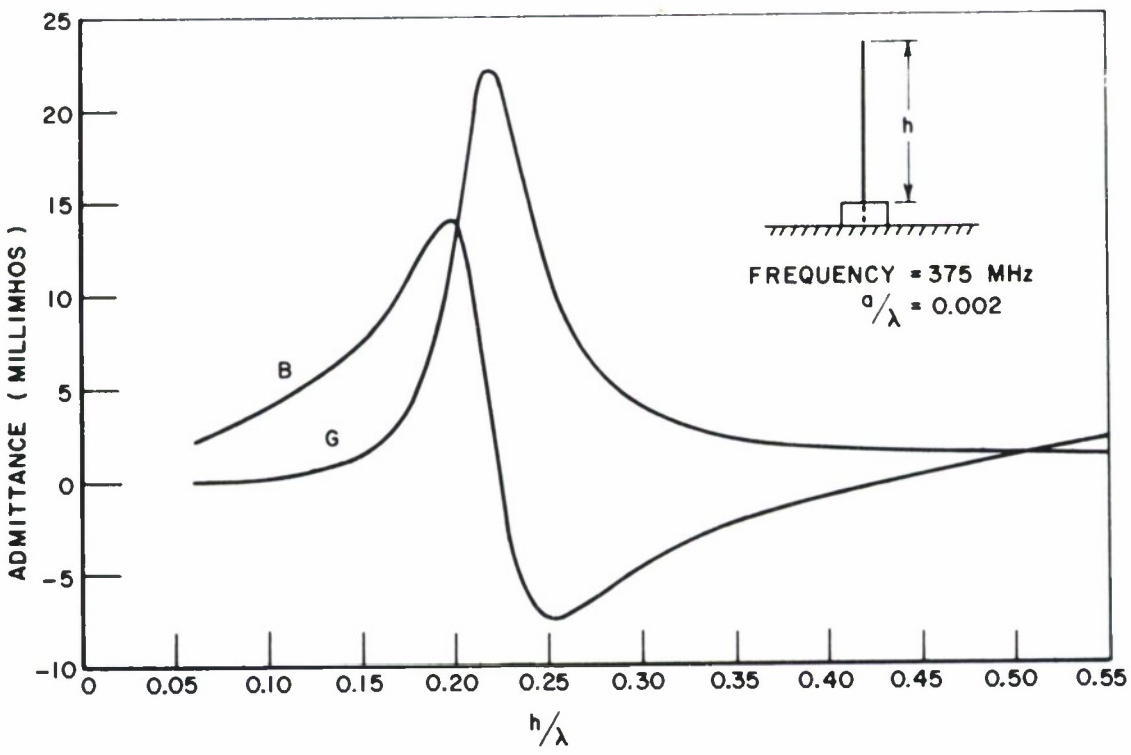

Fig. 12. Measured admittances of modified dipole antenna on small cylindrical shell. (H-P Bridge)

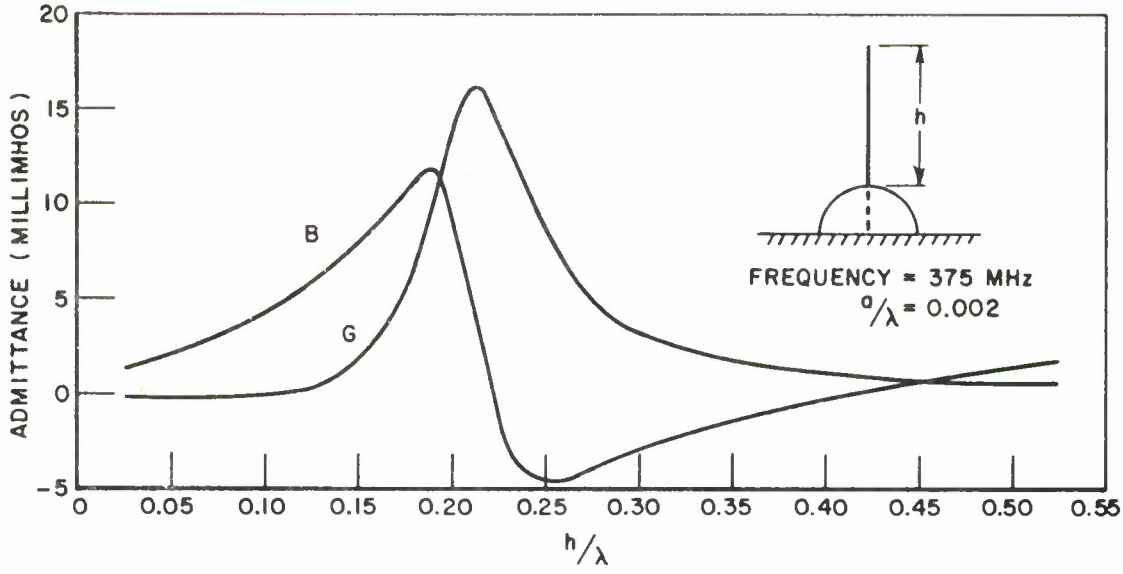

Fig. 13. Measured admittances of modified dipole antenna on large spherical shell. (H-P Bridge)

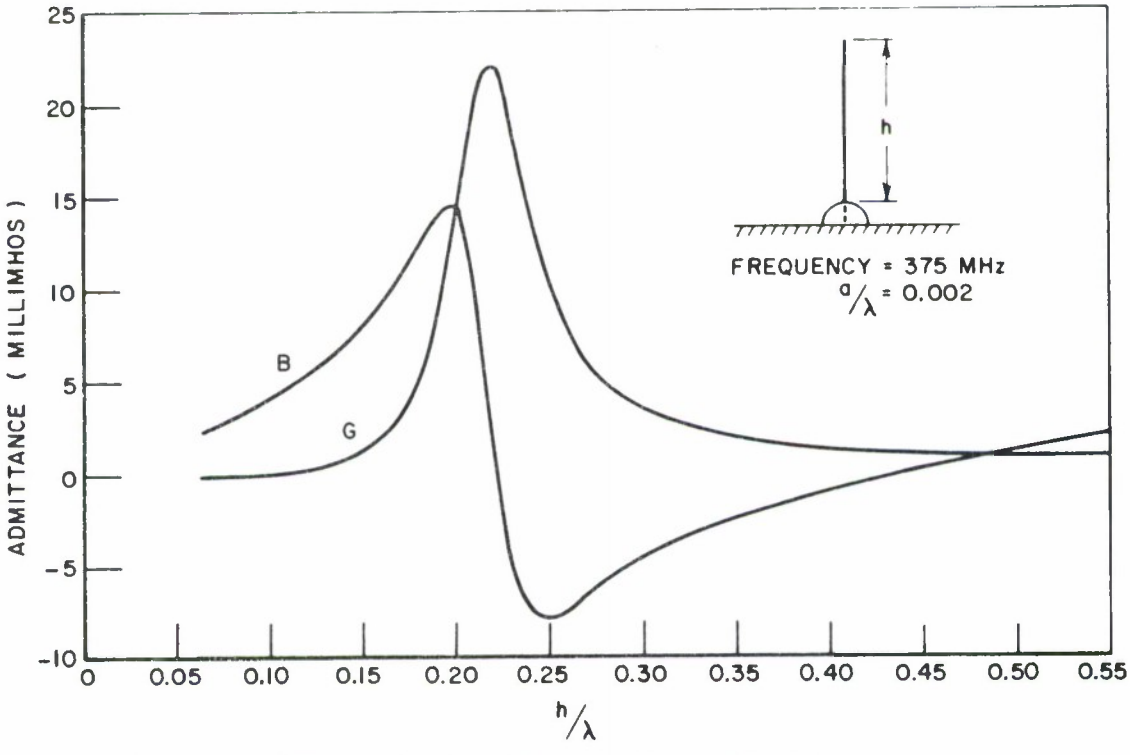

Fig. 14. Measured admittances of modified dipole antenna on small spherical shell. (H-P Bridge)

not change the admittances of the modified antennas by any significant amount.

The measured admittance curves of an unmodified 120° vee-antenna on a large base fitting are shown in Fig. 15. The resonant length occurs at

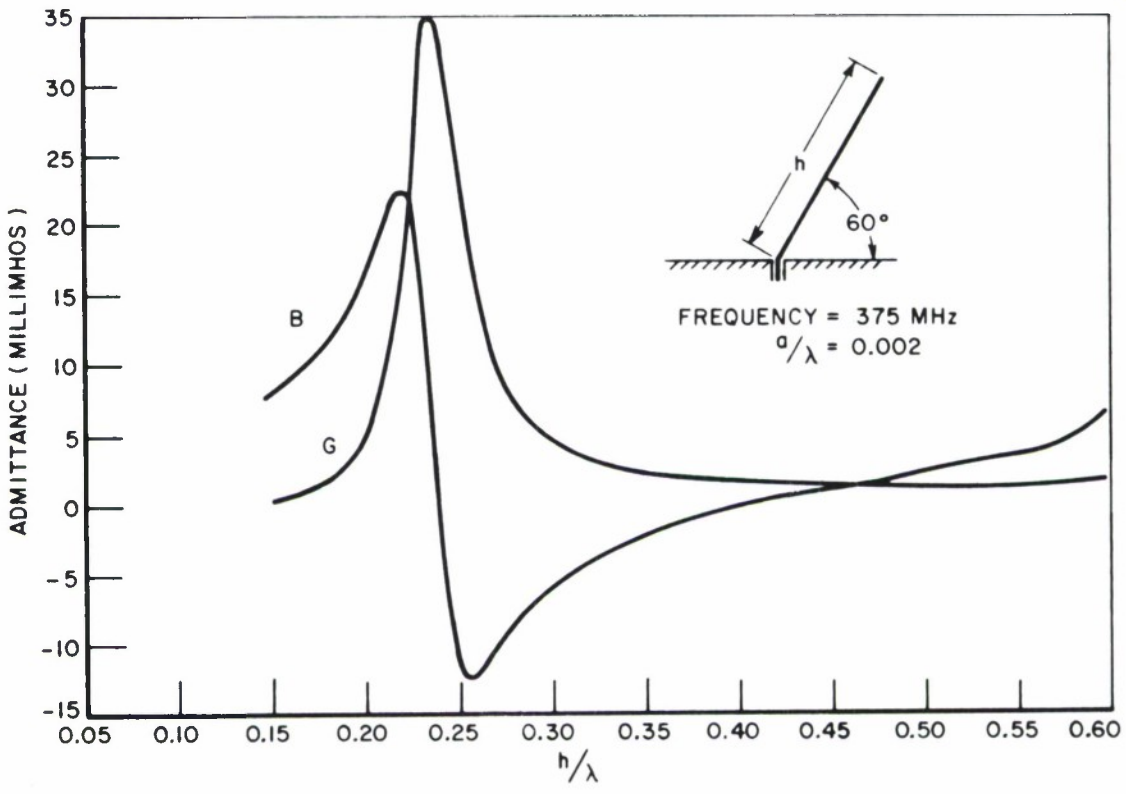

Fig. 15. Measured admittances of 120° vee-antenna on large base fitting. (H-P Bridge)

$h/\lambda = 0.238$ which is higher than that of the monopole antenna on a ground plane. The peak values of the admittance curves in this case are also the highest of all the models.

The measured admittance curves of the modified 120° vee-antenna on large and small spherical shells are shown in Figs. 16 and 17, respectively. The effect of base loading also decreases the resonant lengths and lowers the peaks of the admittance curves for both shell sizes. The admittance curves of the large spherical shell case show the lowest peaks of all with the resonant length at $h/\lambda = 0.221$, whereas for the small case the resonant length is at $h/\lambda = 0.225$.

The measured admittance curves of the 20 cm long vee-antenna on the large base fitting are shown in Fig. 18 as a function of vee angle.

Error Analysis The error in the VHF Bridge is compensated by using the correction graphs provided by the manufacturer. Without correction graphs, the accuracy figures for the bridge specify that the true impedance magnitude will be within: $\pm\left(5 + \frac{\text{frequency(MHz)}}{500}\right)\%$ of the bridge reading and the true impedance phase angle will be within: $\pm\left(3 + \frac{\text{frequency (MHz)}}{500}\right)$ degree of the bridge reading. With the correction graphs, impedance magnitude readings can be corrected to better than $\pm$ 2% and phase angle readings to better than $\pm$ 1.2° over the rated frequency range.

The accuracy of the bridge had been checked prior to making the measurements and the results agreed within the range required by the manufacturer.

Sources of possible inherent errors in the setup are:

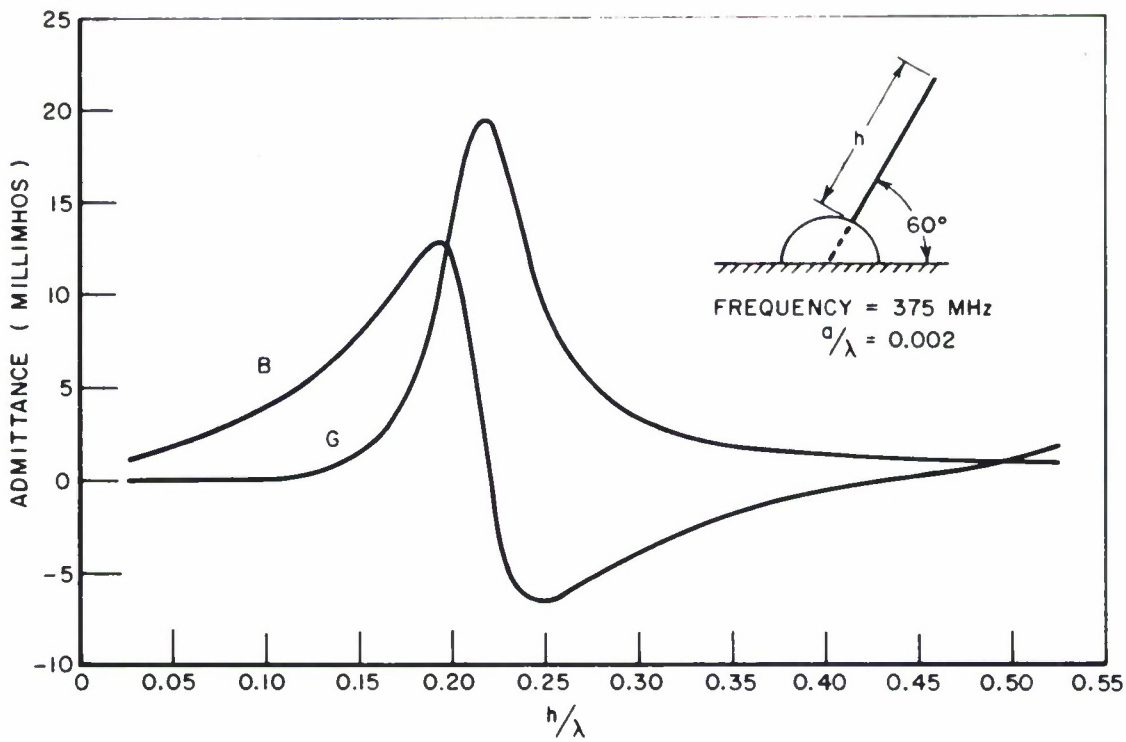

Fig. 16. Measured admittances of modified vee-antenna on large spherical shell. (H-P Bridge)

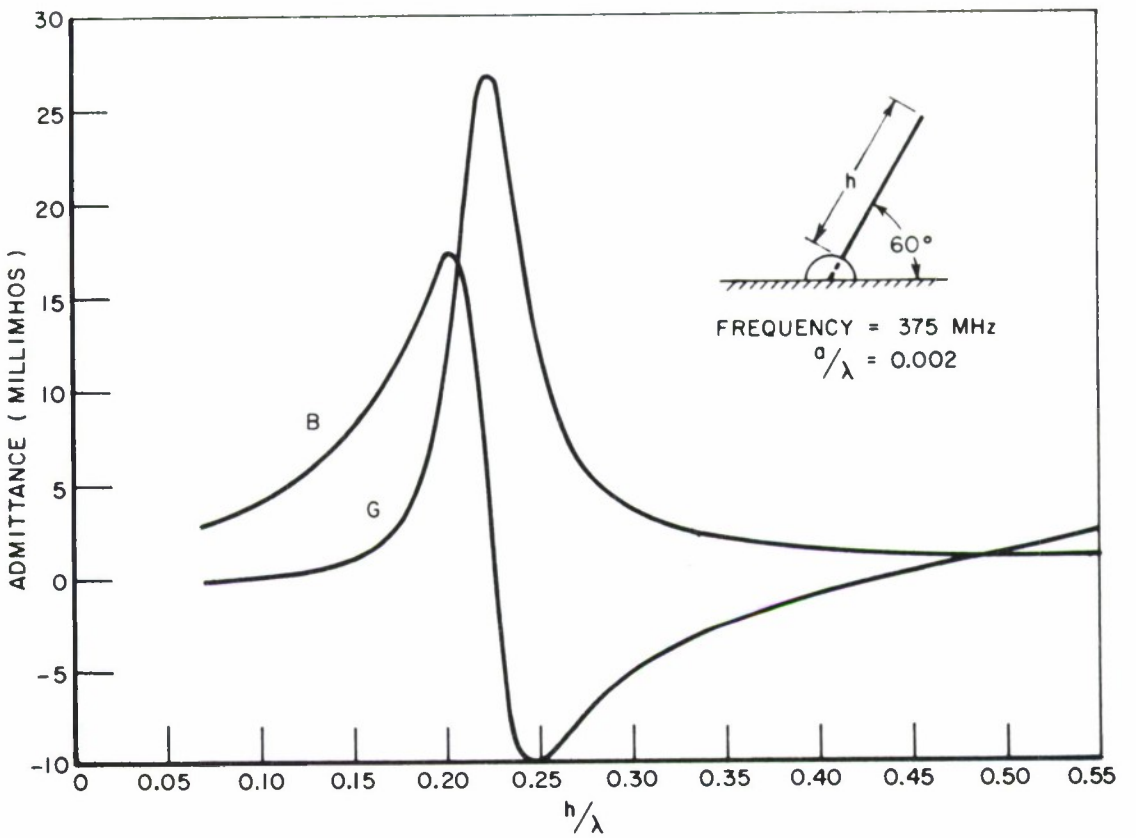

Fig. 17. Measured admittances of modified vee-antenna on small spherical shell. (H-P Bridge)

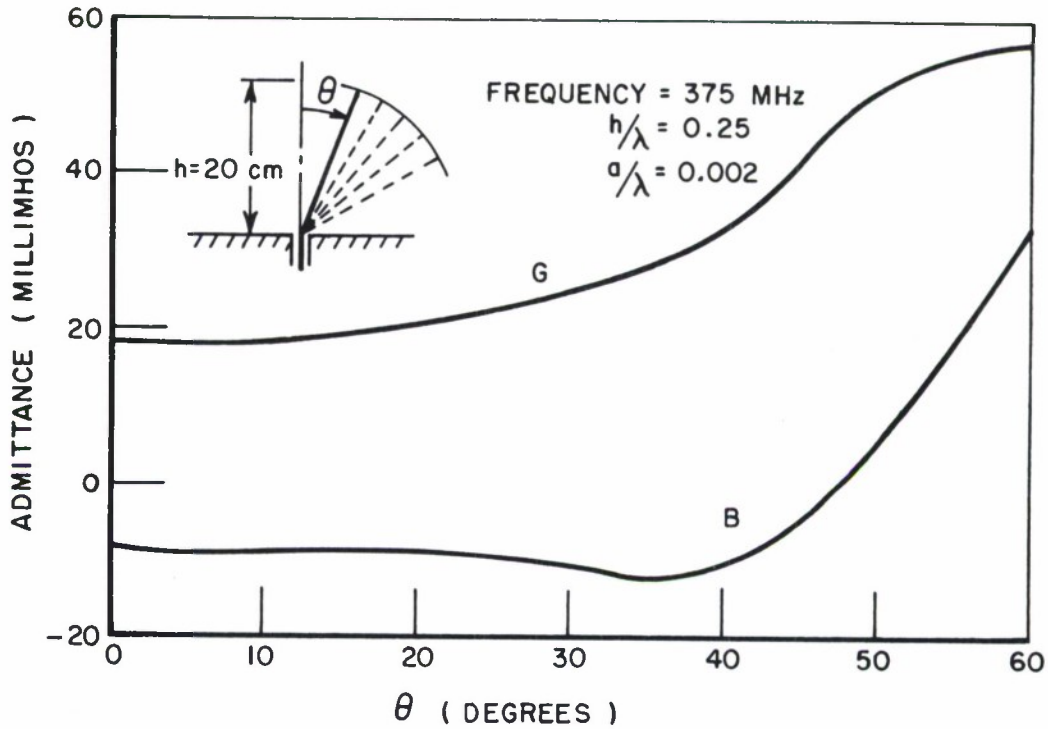

Fig. 18. Measured admittances of 20 cm vee-antenna on large base fitting as a function of vee angle. (H-P Bridge)

1) Discontinuity of the feeding system at the base junction. This is due to the fact that the antenna-mount connector which is a part of the feeding system acts like an air line of slightly different characteristic impedance than 50 ohms, thus introducing a small mismatch. Moreover, a small piece of Teflon ring that is inserted at the tip of the antenna-mount connector near the aperture for centering the antenna wires can cause some changes in the characteristic impedance of the coaxial line.

2) The curvature of the antenna wires caused by gravity and slightly oblique connections when small extension lengths were used.

3) The small ambiguity introduced by nonsharp null. However, this effect was reduced by taking the readings for all cases at least three times independently and the results averaged.

Limitation of the Hewlett-Packard VHF Bridge The impedance magnitude range of the bridge is 2-2,000 ohms. If the line length and frequency of the signal are such that the short is near or at a quarter wavelength point, the impedance magnitude seen by the bridge will be outside the 2-2,000 ohms range. When this condition is encountered, a change in the length of the line is needed to bring the impedance magnitude within the required range.

Phase angle at frequencies other than 100 MHz must be interpolated by the equation: phase angle reading x $\frac{\text{frequency (MHz)}}{100}$ which obviously decreases the accuracy at frequencies much higher than 100 MHz. This makes the upper limit of the frequency for rated accuracy to be 500 MHz. The lower limit of the frequency that gives rated accuracy is 55 MHz and at this frequency and higher the phase angles can be measured from -90° to $+90^{\circ}$. However, the bridge can be used at frequencies down to 5 MHz and up to 1,000 MHz with decreased accuracy. The maximum measurable phase angle at 5 MHz is -8.8° to $+8.8^{\circ}$.

CHAPTER III
RADIATION PATTERN MEASUREMENTS

A. Model Constructions

Radiation patterns of the modified dipole antennas with large cylindrical and spherical shell sizes were measured at 9 different antenna wire lengths around the resonant region. The details of the model constructions are shown in Fig. 19. The cylindrical and spherical shells are made of aluminum and each shell consists of two halves assembled together by a one turn mating thread. Two 1/16" diameter holes, 1/2" apart are drilled through the shells of both geometries near the splitting lines for running out a parallel-wire transmission line. Provision for interchangeability of antenna wires is also available through receptacle male screws in the shells which mate the female threads on the antenna wires. Photographs of antenna models and pattern measuring arrangement are shown in Fig. 20.

B. Pattern Measurement Arrangements

Referring to Fig. 21 $E_\theta(\theta)$ patterns of the modified dipole antennas were measured with the antennas under test operated as receivers. The schematic diagram of the measuring arrangement is shown in Fig. 22, the photograph of the pattern measurement range is shown in Fig. 20(a). The transmitting antenna used was a log-periodic type operated at 375 MHz, and was fixed in horizontal position at the height of 5.68 m above

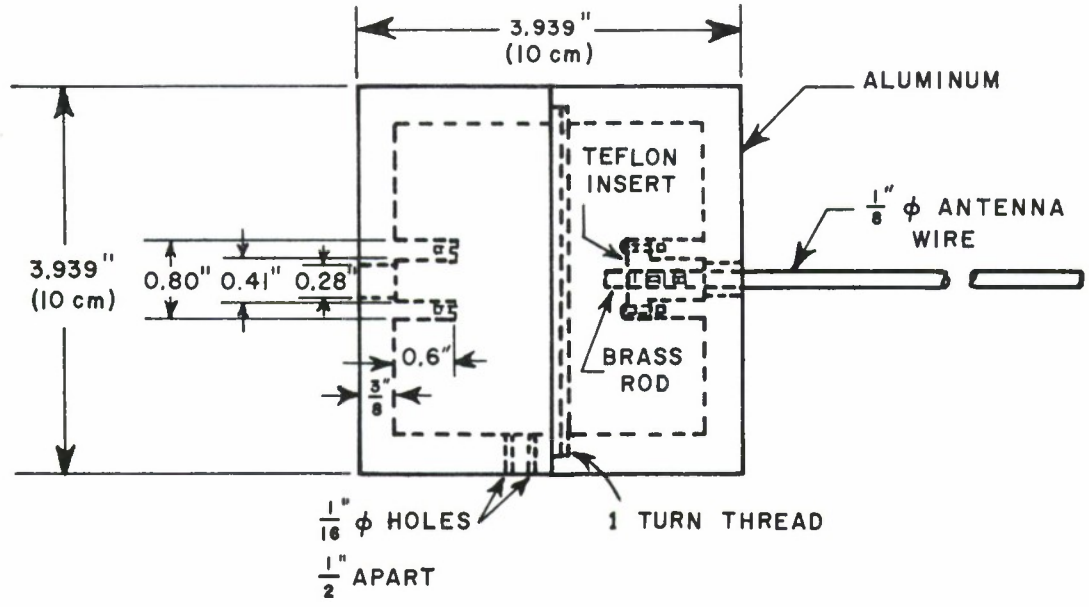

(a) MODIFIED DIPOLE ANTENNA WITH CYLINDRICAL SHELL

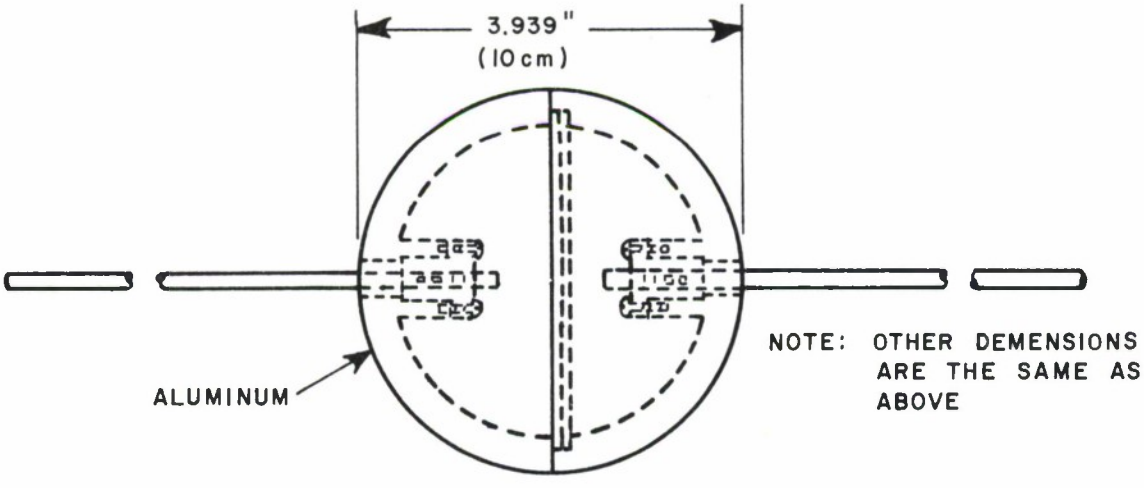

(b) MODIFIED DIPOLE ANTENNA WITH SPHERICAL SHELL

Fig. 19. Details of model constructions for pattern measurements.

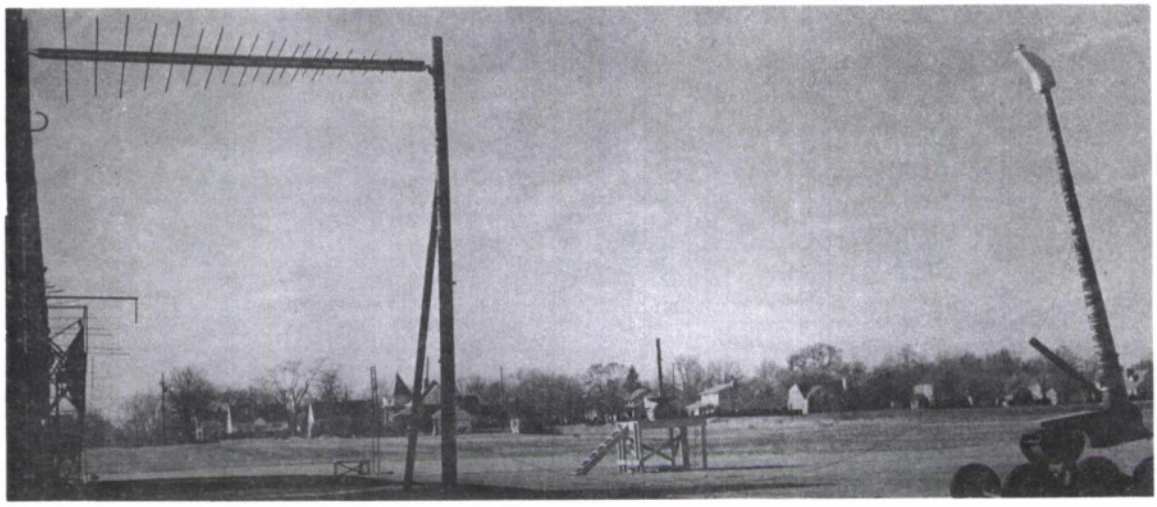

(a) PATTERN MEASUREMENT RANGE

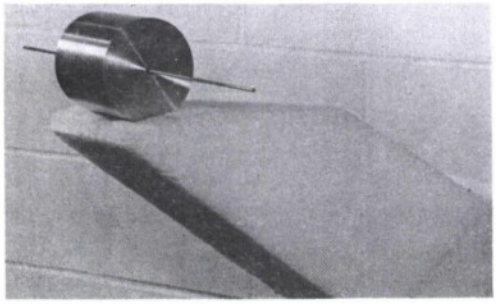

(b) MODIFIED DIPOLE ANTENNA WITH CYLINDRICAL SHELL

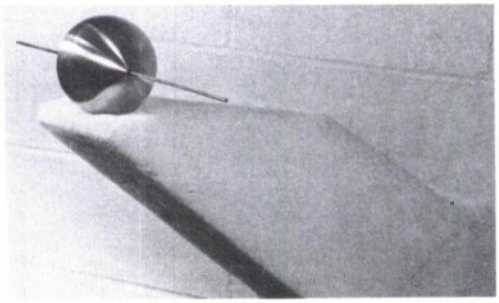

(c) MODIFIED DIPOLE ANTENNA WITH SPHERICAL SHELL

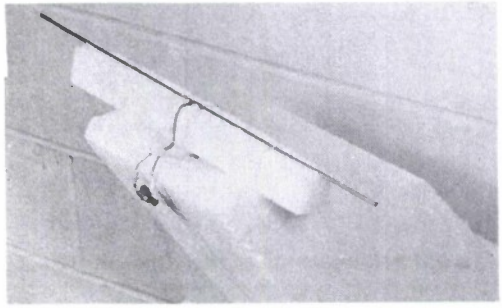

(d) HALF-WAVE DIPOLE ANTENNA

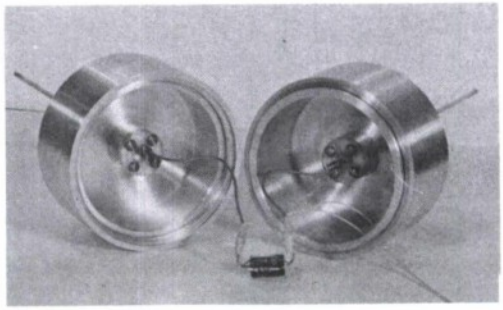

(e) INSIDE CONSTRUCTION AND DIODE DETECTOR CIRCUIT OF MODIFIED DIPOLE ANTENNA

Fig. 20. Photographs of models for far field pattern measurements.

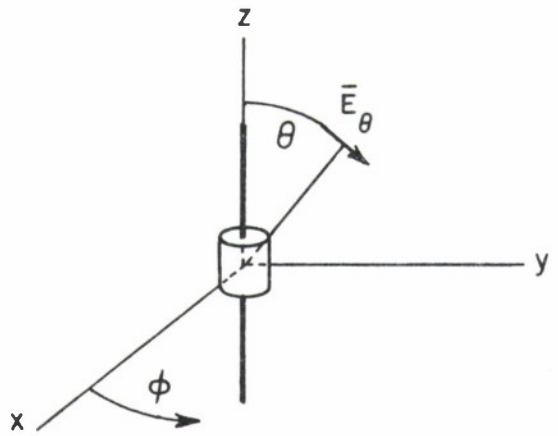

Fig. 21. Relations for pattern measurements of modified dipole antenna.

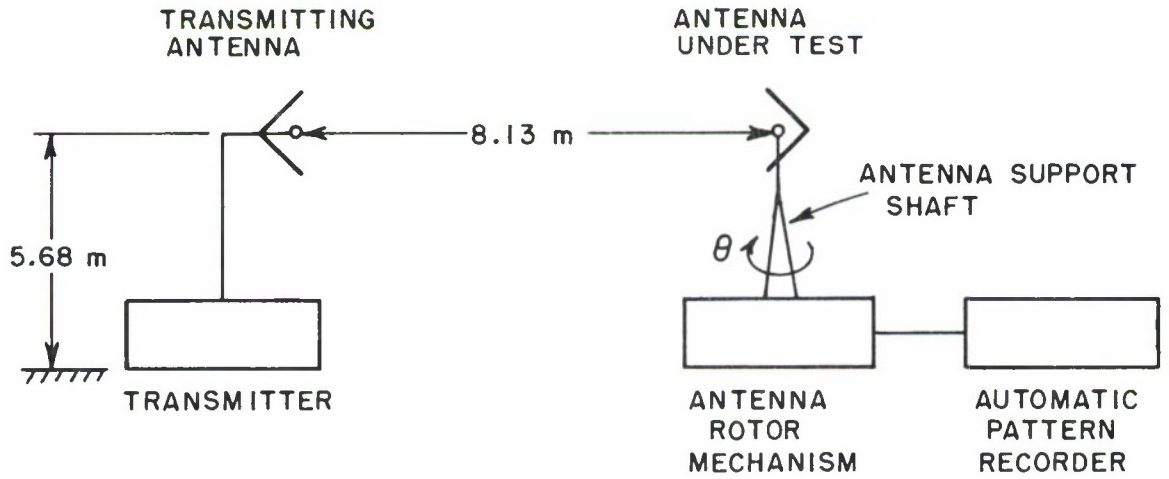

Fig. 22. Antenna pattern measuring arrangement.

ground level. The modified dipole antenna under test was placed in horizontal position on a styrofoam support attached to the top of the antenna support shaft, as shown in Figs. 20(b) and (c), at practically the same height as the transmitting antenna and at 8.13 m apart. The received signals from the modified dipole antenna were fed to the Antlab Model 3309-7 Automatic Pattern Recorder and were recorded on rectangular coordinate papers.

C. Detector Circuit

Since the antenna under test was operated as a receiver, a diode detector circuit was placed inside the metallic shell of the modified dipole antenna, as a receiver, as shown in Fig. 20(e). The circuit diagram of the diode detector is shown in Fig. 23. With the selected

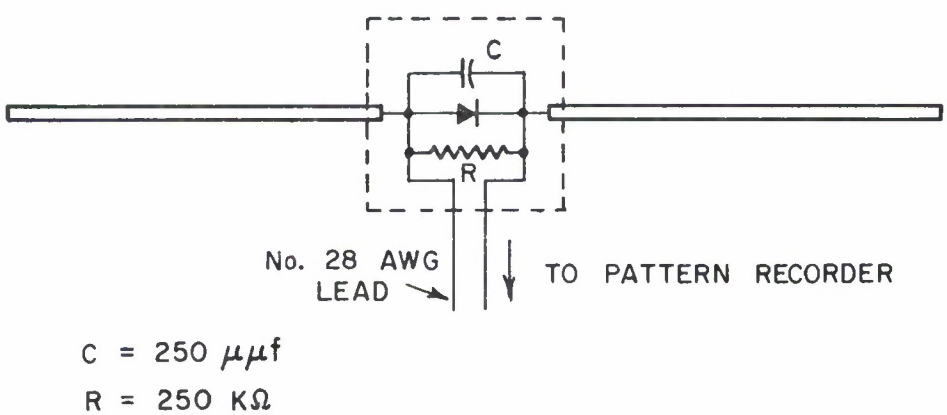

Fig. 23. Diode detector circuit.

values of R and C, the diode detector was used to detect the 375 MHz signals modulated at 500 Hz received by the modified dipole antenna. The 500 Hz detected signals were brought out of the metallic shell by a pair of No. 28 AWG leads which ran through the holes provided in the shells. The parallel wire transmission line had extremely small wire radius and was kept practically perpendicular to the antenna so that its presence had insignificant effect on antenna's characteristics. Detection inside the shells guaranteed that the transmission line would not reradiate since the signals appearing in the line were at audio frequency. The No. 28 AWG parallel line was continued for three feet away from the antenna before it was connected to a coaxial cable which in turn is connected to the automatic pattern recorder.

D. Checking the Pattern Recording Range

A half wave dipole antenna at the operating frequency of 375 MHz, consisting of a pair of 1/8" diameter brass rods with a minimum feeding gap width was measured on the range using the same diode detector circuit connected at the feed point as shown in Fig. 20(d). The patterns were recorded on both linear and log scales as shown in Figs. 24 and 25, respectively. Only half of the patterns are shown because of the symmetry. The corresponding beamwidths are 79.2° and 78.6° as compared to 78° by an analysis assuming sinusoidal current distribution.[7] Calibration of the recorded power levels at the pattern recorder was done through the use of a Weinschel Engineering Model 905, r-f attenuator. The calculated pattern is also plotted in Figs. 24 and 25 for comparison.

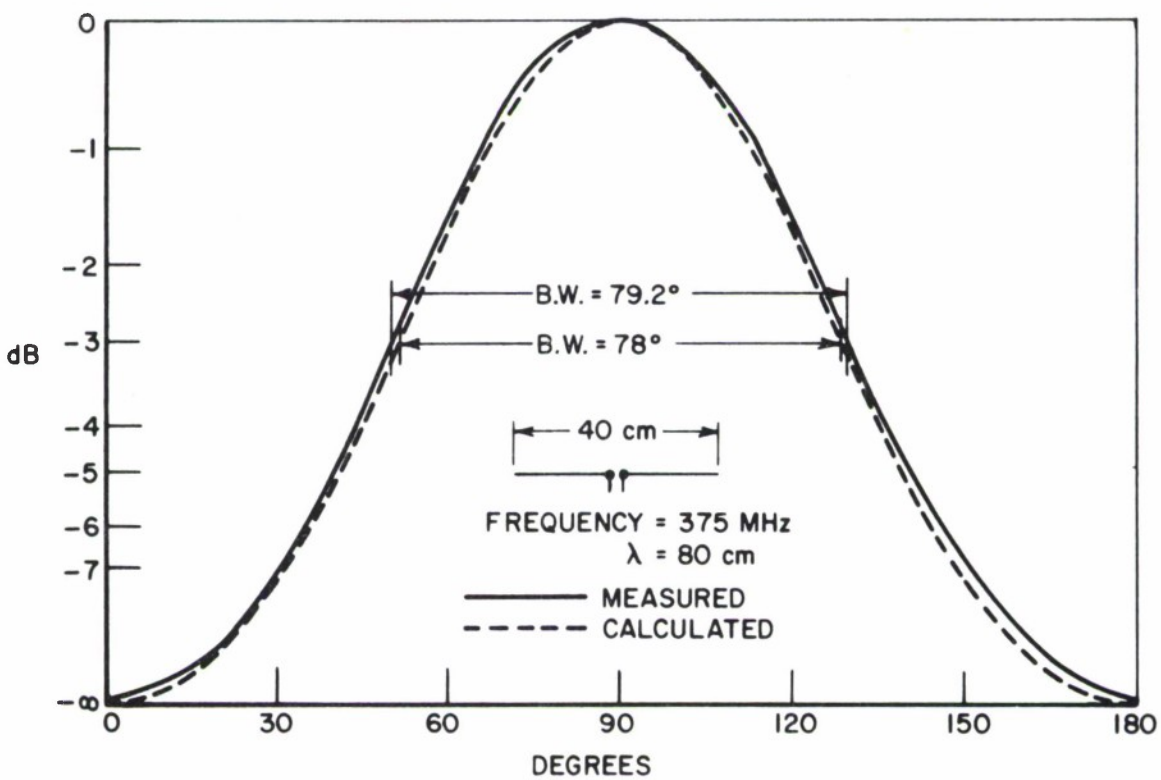

Fig. 24. Comparison between measured and calculated power patterns of a halfwave dipole antenna.

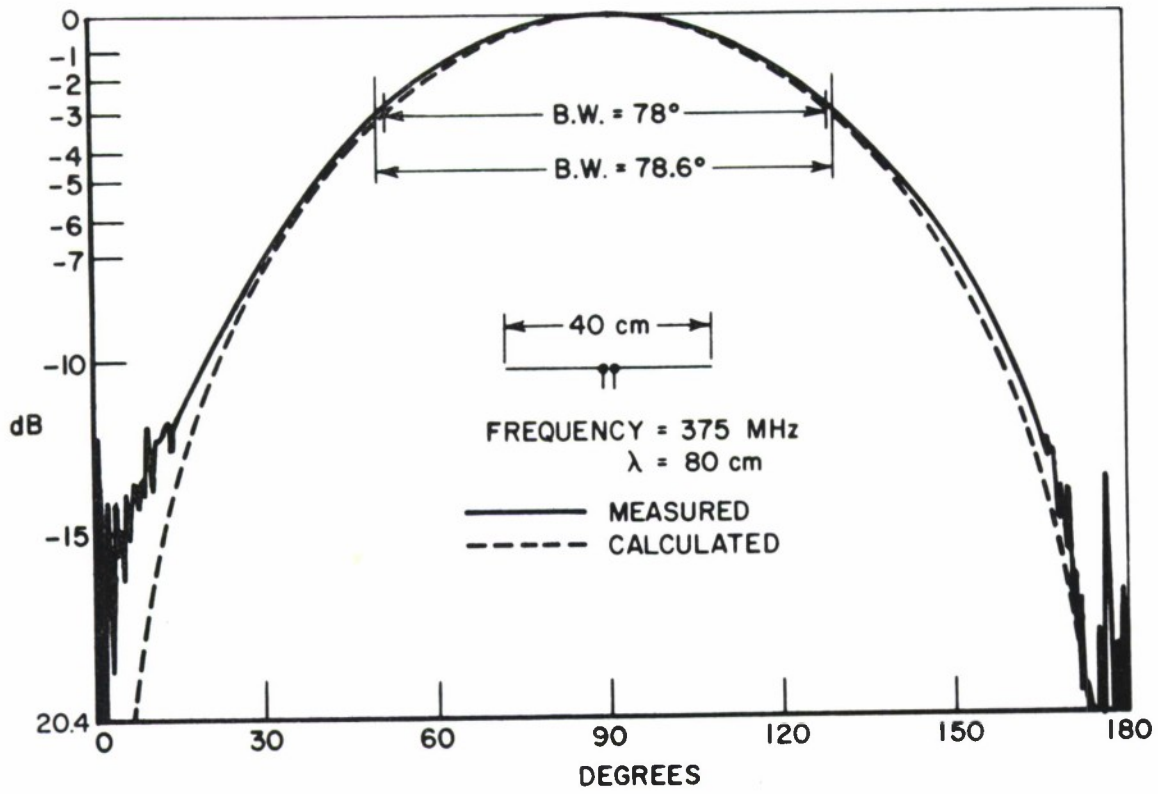

Fig. 25. Comparison between measured and calculated $E_\theta(\theta)$ patterns of a halfwave dipole antenna.

The measured and calculated patterns conform very well. This check assures us of a good accuracy in pattern measurements using the same procedures.

E. Measured Results

The measured patterns on linear and log scales of the modified dipole antenna with cylindrical shell at resonant length, i.e., at 46.2 cm overall length as deduced from admittance curves in Fig. 11, are

shown in Figs. 26 and 27, respectively. Only half of the patterns are shown because of the symmetry. The patterns have a beamwidth of about $77\frac{1}{4}^{o}$. Also plotted on both log and linear scales in Figs. 26 and 27, for comparsion, is the calculated pattern of a 46.2 cm dipole antenna. The beamwidth of this calculated pattern is 74.6^{o}. The overall shape of the measured patterns on both linear and log scales conform very well to the calculated pattern.

The measured patterns of the modified dipole antenna with spherical shell at resonance, i.e., at 45.6 cm overall length as deduced from admittance curves in Fig. 13, are shown in Figs. 28 and 29 with the beamwidth of about $76\frac{1}{2}^{o}$. Comparison with the calculated pattern is also made in the same way as in the cylindrical case. The beamwidth of this calculated pattern is 75°. The overall shape of the measured patterns also conform very well to the calculated pattern.

Measured radiation patterns of both modified dipole antennas at other antenna wire lengths are not shown since they all have basically the same shape although with different beamwidths.

The measured and calculated values of beamwidth and directivity are compared in Table 1 at 9 different antenna wire lengths around resonance. For a doughnut-type pattern, directivity is given by $D = 114.6/\theta^{o}$ where θ^{o} is the beamwidth.

It is obvious from Table 1 that the presence of metallic shells increases the beamwidth for the modified dipole antenna at the overall lengths L greater than $\lambda/2$, while at shorter lengths, the beamwidths of both measured and calculated patterns are practically the same. Re-

TABLE 1
COMPARISON OF THE BEAMWIDTHS AND DIRECTIVITIES BETWEEN MEASURED PATTERNS OF MODIFIED DIPOLE ANTENNAS AND CALCULATED PATTERNS OF A DIPOLE ANTENNA

L (CM)	$\frac{L}{\lambda}$ (λ = 80 cm)	MEASURED				CALCULATED		Current Distributions
		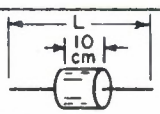		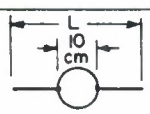				
		B. W.	D.	B. W.	D.	B. W.	D.	
31.0	0.3875	83.1°	1.378	82.4°	1.391	82.0°	1.398	
35.0	0.4375	79.08°	1.45	81.9°	1.40	81.0°	1.415	
40.0	0.5000	77.4°	1.48	77.86°	1.472	78.0°	1.47	$L = \frac{\lambda}{2}$
45.6	0.5700	77.28°	1.483	77.44°	1.782	75.0°	1.528	
46.2	0.5775	77.22°	1.485	76.2°	1.503	74.6°	1.536	
50.0	0.625	72.28°	1.586	73.28°	1.564	70.8°	1.618	
59.0	0.7375	67.53°	1.696	67.51°	1.697	64.8°	1.768	
67.0	0.8385	63.24°	1.811	63.0°	1.82	58.4°	1.962	
75.0	0.9375	58.74°	1.95	56.73°	2.02	51.8°	2.21	

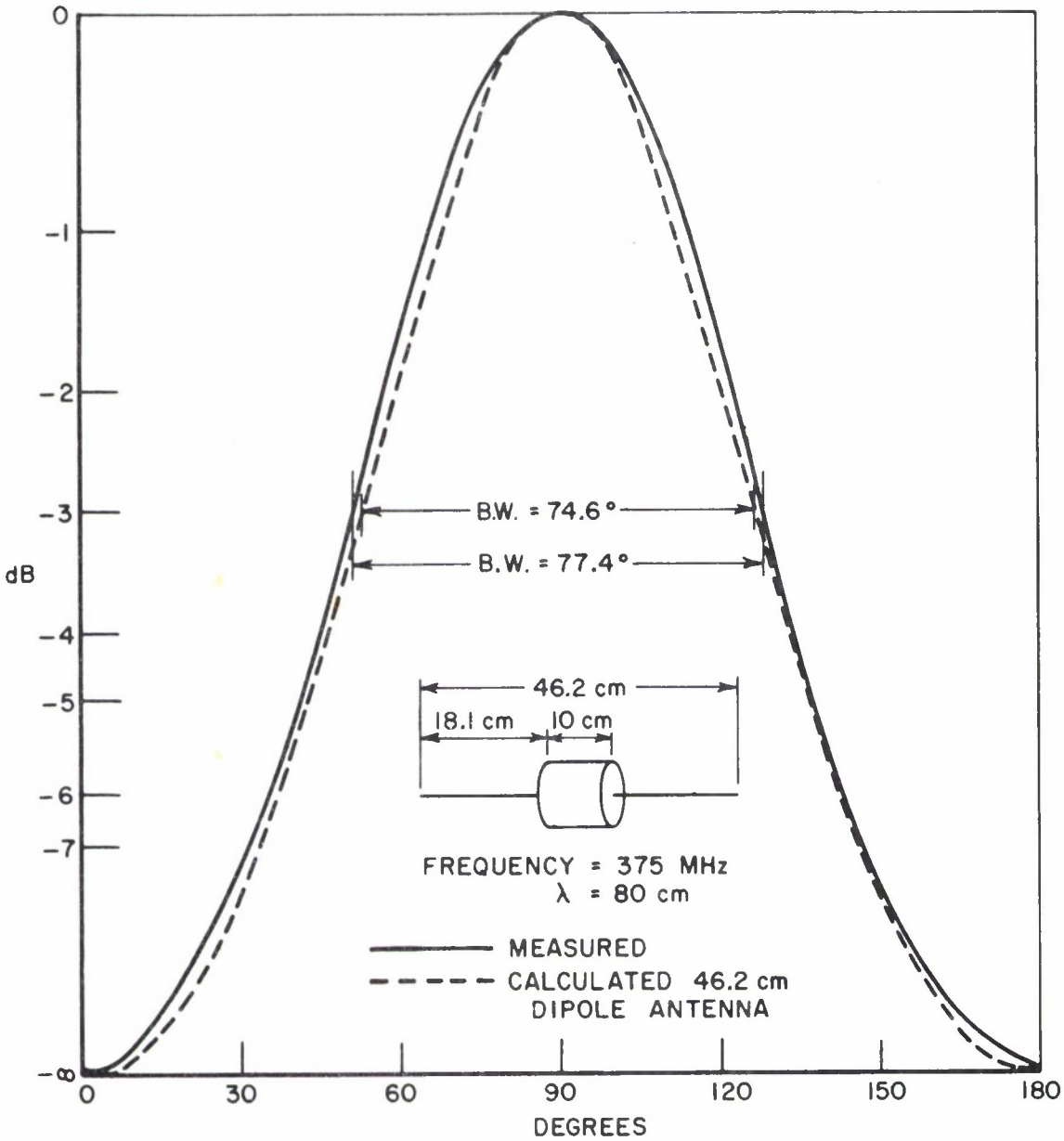

Fig. 25. Comparison between measured power pattern of the modified dipole antenna with cylindrical shell at resonance and calculated pattern of a dipole antenna at the same overall length.

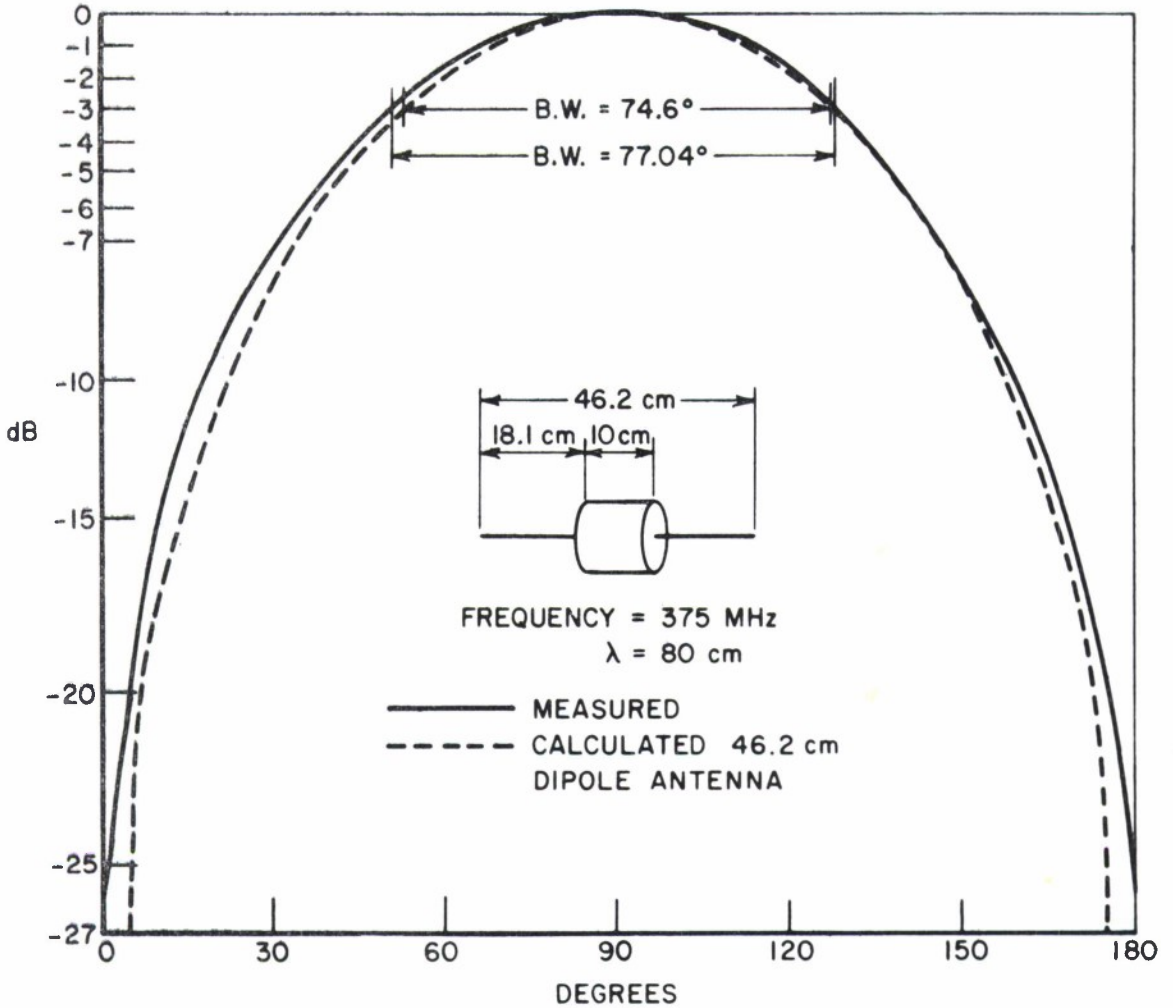

Fig. 26. Comparison between measured $E_\theta(\theta)$ pattern of the modified dipole antenna with cylindrical shell at resonance and calculated pattern of a dipole antenna at the same overall length.

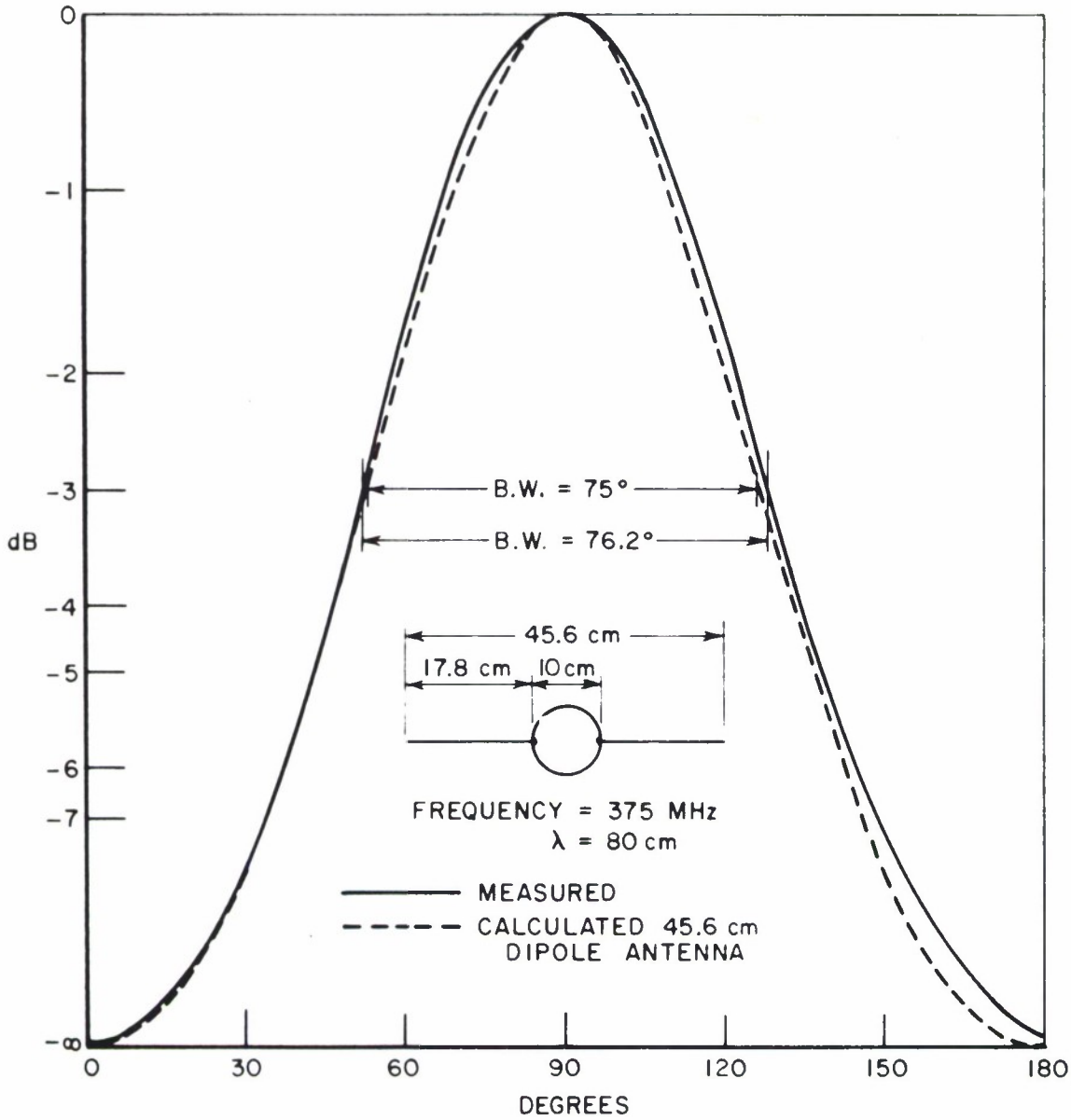

Fig. 27. Comparison between measured power pattern of the modified dipole antenna with spherical shell at resonance and calculated pattern of a dipole antenna at the same overall length.

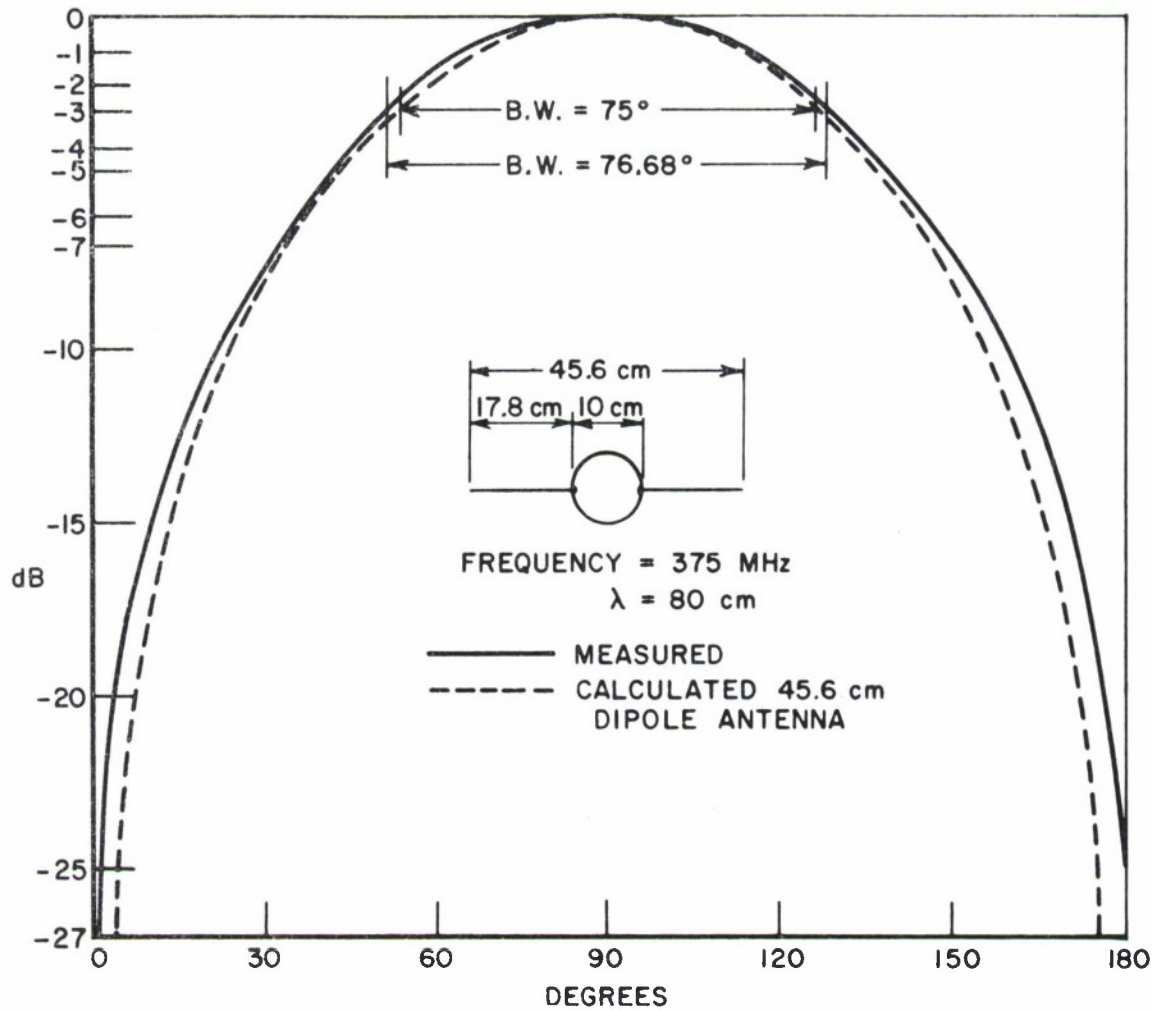

Fig. 28. Comparison between measured $E_\theta(\theta)$ pattern of the modified dipole antenna with spherical shell at resonance and calculated pattern of a dipole antenna at the same overall length.

ferring to Table 1 it is seen that whenever the current distributions at the feed points of dipole antennas are maximum, such as at $L \leqq \lambda/2$, the calculated beamwidths are nearly the same as the measured results. But when the current distributions at the feed points are lower than the other points, such as at $L \geqq \lambda/2$, the calculated beamwidths are

narrower than the measured results. This shows that the realistic current distributions on both metallic shells of the modified dipole antennas are higher than assumed in the sinusoidal distribution.

The gain of the modified dipole antennas cannot readily be measured since the antennas were not matched to the transmission line. The impedance of the diode detector circuit when combined in parallel with the impedance of the antenna itself gives rise to a certain value of impedance at each antenna wire length. In this arrangement, the maximum power transfer happened to occur at the overall length of 55 cm.

CHAPTER IV
CONCLUSIONS

The admittance curves of the modified and unmodified dipole antennas behave similarly with the values of conductance maximum near resonant lengths; the values of susceptance are maximum at lower than resonant lengths and minimum at longer than resonant lengths. For admittance measurements, the height of the modified antennas are referred to the aperture where the antenna wire enters the shell. The admittance is also referred to this point. Using this reference, base loading of the dipole and vee-antennas by cylindrical and spherical shells lowers the peak values and slightly lowers the resonant lengths from the unmodified cases. In general, changes in admittance peaks due to the shells are large and more sensitive to the size than to the geometry of the shells, whereas the change in resonant length is small and is almost constant for all sizes and geometries of the shell. For the modified dipole and vee-antennas with large size shells, admittance peaks are only at 40% to 70% of the unmodified cases, but for the small size shells, admittance peaks are higher, i.e., at 80% to 90% of the unmodified cases. Resonant lengths for all cases are shortened by the amount of 4% to 8% from the unmodified cases. Although the admittance peaks of the modified dipole antennas are almost the same for the cases of small cylindrical and spherical shells, the admittance peaks of the

large cylindrical shell case can still be observed to be 5% to 20% lower than that of the large spherical case.

If the resonant lengths of the modified antennas are measured with respect to the ground planes instead of to the apertures as they are now measured, the effect of base loading must be regarded as lengthening the resonant lengths because the shell radius must be added to all of the original lengths, making the total lengths longer than the resonant length of the unmodified cases. With this new reference, the larger the shell sizes, the longer the resonant lengths of both the modified dipole and vee-antenna cases.

The radiation patterns of the modified dipole antennas on large cylindrical and spherical shells are practically the same and are similar to the patterns of a conventional dipole. However, by the effect of metallic shells at the centers, the beamwidths of the measured patterns at the overall antenna lengths greater than $\lambda/2$ have the tendency to be broader than those of conventional dipoles due to a current distribution on the metallic shell which is different than that of a conventional dipole. At antenna lengths less than or equal to $\lambda/2$, the beamwidths of the modified and unmodified dipole antennas are almost the same.

Cross polarization in both models was also checked in this experiment but the effect appeared to be negligible.

APPENDIX A
TRANSFORMATION OF IMPEDANCES FROM BRIDGE REFERENCE TO APERTURE PLANE USING TRANSMISSION LINE THEORY

Consider the transmission line circuit shown above. The characteristic impedance is Z_o (complex in general); the propagation constant is $\gamma = \alpha + j\beta$; and the length is ℓ. The line is terminated in complex impedance Z_L. The impedance Z_{IN} observed at the end of the line is given by Moore[8] as

$$(3) \qquad \frac{Z_{IN}}{Z_o} = \frac{1 + \rho\, e^{-2\gamma\ell}}{1 - \rho\, e^{-2\gamma\ell}}$$

where

$$(4) \qquad \rho = \frac{Z_L - Z_o}{Z_L + Z_o} \quad .$$

If the load end is short circuited, i.e., $Z_L = 0$, then $Z_{IN} = Z_{SC}$ and $\rho = -1$. Hence

$$(5) \qquad \frac{Z_{SC}}{Z_o} = \frac{1 - e^{-2\gamma\ell}}{1 + e^{-2\gamma\ell}}$$

or

$$(6) \qquad e^{-2\gamma\ell} = \frac{1 - \dfrac{Z_{SC}}{Z_o}}{1 + \dfrac{Z_{SC}}{Z_o}}$$

Substitute (4) and (6) in (3) we have:

$$(7) \qquad \frac{Z_L}{Z_o} = \frac{1 + \dfrac{\left(1 + \dfrac{Z_{SC}}{Z_o}\right)\left(\dfrac{Z_{IN}}{Z_o} - 1\right)}{\left(1 - \dfrac{Z_{SC}}{Z_o}\right)\left(\dfrac{Z_{IN}}{Z_o} + 1\right)}}{1 - \dfrac{\left(1 + \dfrac{Z_{SC}}{Z_o}\right)\left(\dfrac{Z_{IN}}{Z_o} - 1\right)}{\left(1 - \dfrac{Z_{SC}}{Z_o}\right)\left(\dfrac{Z_{IN}}{Z_o} + 1\right)}} .$$

But $Z_o = 50$ ohms and $Y_L = 20 \dfrac{Z_o}{Z_L}$ millimhos. Hence

$$(8) \quad Y_L = 20 \; \frac{1 - \dfrac{\left(1 + \dfrac{Z_{SC}}{50}\right)\left(\dfrac{Z_{IN}}{50} - 1\right)}{\left(1 - \dfrac{Z_{SC}}{50}\right)\left(\dfrac{Z_{IN}}{50} + 1\right)}}{1 + \dfrac{\left(1 + \dfrac{Z_{SC}}{50}\right)\left(\dfrac{Z_{IN}}{50} - 1\right)}{\left(1 - \dfrac{Z_{SC}}{50}\right)\left(\dfrac{Z_{IN}}{50} + 1\right)}} \quad \text{millimhos.}$$

APPENDIX B
COMPUTER PROGRAM FOR HEWLETT-PACKARD BRIDGE MEASUREMENTS

The dial readings from Hewlett-Packard VHF Bridge are listed as $Z_{SCM} \underline{|Z_{SCP}}$ and $Z_{INM} \underline{|Z_{INP}}$. By using correction graphs specific to this instrument provided by the manufacturer, the corrected values of $Z_{SCM} \underline{|Z_{SCP}}$ and $Z_{INM} \underline{|Z_{INP}}$ are listed as Z_{SC} and Z_{IN}, where

(9) $$Z_{SC} = Z_{SCM} \{0.977 + 0.01|\sin (Z_{SCP} \times 3\ 75)|(^{1.8*}_{2.8})\}$$

$$\cdot [\cos\{Z_{SCP} \cdot (^{3.84*}_{3.91}) + 0.75\} + j\sin \{Z_{SCP} \cdot (^{3.84*}_{3.91}) + 0.75\}]$$

(10) $$Z_{IN} = Z_{INM} \{0.977 + 0.01|\sin(Z_{INP} \times 3.75)|(^{1.8*}_{2.8})\}$$

$$\cdot [\cos\{Z_{INP} \cdot (^{3.84*}_{3.91}) + 0.75\} + j\sin\{Z_{INP} \cdot (^{3.84*}_{3.91}) + 0.75\}]$$

The admittance Y_L at the short circuit point can be calculated from Eq. (8) of Appendix A.

---

* The upper figures are used when Z_{SCP} and Z_{INP} are positive angles, and the lower figures are used when Z_{SCP} and Z_{INP} are negative angles.

$$Y_L = 20 \frac{1 - \dfrac{\left(1 + \dfrac{Z_{SC}}{50}\right)\left(\dfrac{Z_{IN}}{50} - 1\right)}{\left(1 - \dfrac{Z_{SC}}{50}\right)\left(\dfrac{Z_{IN}}{50} + 1\right)}}{1 + \dfrac{\left(1 + \dfrac{Z_{SC}}{50}\right)\left(\dfrac{Z_{IN}}{50} - 1\right)}{\left(1 - \dfrac{Z_{SC}}{50}\right)\left(\dfrac{Z_{IN}}{50} + 1\right)}} \text{ millimhos.}$$

The computer program using the IBM 7094 computer and PUFFT compiler for calculation of Y_L with $Z_{SCM}\underline{|Z_{SCP}}$ and $Z_{INM}\underline{|Z_{INP}}$ as inputs is shown below.

```
        $EXECUTE                PUFFT
$PUFFT   200
PUFFT   VERSION 10/24/66
        COMPLEX ZSC,ZIN,YL,C1,C2
        RA=57.29578
        READ (5,10) N1
10      FORMAT(I5)
        DO 60 I=1,N1
11      READ (5,12) ZSCM,ZSCP,N2
12      FORMAT (2F10.4,I5)
        TEMP1=1.8
```

```
      TEMP2=3.84
      IF (ZSCP.GT.0.) GO TO 13
      TEMP1=2.8
      TEMP2=3.91
13    TEMP=(ZSCP*TEMP2+0.75)/RA
      ZSC =ZSCM/50.*(0.977+0.01*ABS(SIN(ZSCP*3.75/RA))*TEMP1)*CMPLX(COS(T
     2EMP),SIN(TEMP))
      C1=(1.0+ZSC)/(1.0-ZSC)
      WRITE (6,14) ZSC
14    FORMAT (20X,4HZSC=,2E15.7///14X,1HH,30X,3HZIN,37X,2HYL/)
      DO 50 J=1,N2
      READ (5,20) H,ZINM,ZINP
20    FORMAT (3F10.4)
      TEMP1=1.8
      TEMP2=3.84
      IF(ZINP.GT.0.) GO TO 25
      TEMP1=2.8
      TEMP2=3.91
25    TEMP=(ZINP*TEMP2+0.75)/RA
      ZIN=ZINM/50.*(0.977+0.01*ABS(SIN(ZINP*3.75/RA))*TEMP1)*CMPLX(COS(T
     2EMP),SIN(TEMP))
      C2=(ZIN-1.0)/(ZIN+1.0)
      YL=20.0*(1.0-C1*C2)/(1.0+C1*C2)
      WRITE (6,30) H,ZINM,ZINP,YL
30    FORMAT (10X,F10.4,10X,2E15.7,10X,2E15.7)
```

```
50      CONTINUE
60      CONTINUE
        STOP
        END
$DATA
```

REFERENCES

1. Otto, D.V., University of Auckland, New Zealand, private communications.
2. Otto, D.V., "The Admittance of Cylindrical Antennas Driven from a Coaxial Line," Radio Science 2 (New Series) No. 9, September, 1967, pp. 1031-1042.
3. Otto, D.V., "Fourier Transform Method in Cylindrical Antenna Theory," Radio Science 3 (New Series) No. 11, November, 1968, pp. 1050-1057.
4. Mack, R.B., "A Study of Circular Arrays," Part 1-3, Technical Report, Nos. 381-383, May 1, 1963, Cruft Laboratory, Harvard University, Cambridge, Mass.
5. Richmond, J.H., "Theoretical Study of V-Antenna Characteristics for the ATS-E Radio Astronomy Experiment," Report 2619-1, The Ohio State University, February 1969, prepared under Contract NAS5-11543, National Aeronautics and Space Administration.
6. Hewlett-Packard Company, "Operating and Service Manual for Model 803A VHF Bridge Serial 112," Hewlett-Parkard Company, March 1962.
7. Kraus, J.D., Antennas, McGraw-Hill Book Company, Inc., New York, 1950, pp. 139-142.
8. Moore, R.K., Traveling Wave Engineering, McGraw-Hill Book Company, Inc., New York, 1960, p. 143.

DOCUMENT CONTROL DATA – R&D

(Security classification of title, body of abstract and indexing annotation must be entered when the overall report is classified)

1. ORIGINATING ACTIVITY *(Corporate author)*
Ohio State University Electroscience Laboratory
under Purchase Order C-781 to Lincoln Laboratory, M.I.T.

2a. REPORT SECURITY CLASSIFICATION
Unclassified

2b. GROUP
None

3. REPORT TITLE
An Experimental Investigation of Modified Dipole Antennas

4. DESCRIPTIVE NOTES *(Type of report and inclusive dates)*
Technical Report

5. AUTHOR(S) *(Last name, first name, initial)*
Lekhyananda, Danai

6. REPORT DATE
2 July 1969

7a. TOTAL NO. OF PAGES
58

7b. NO. OF REFS
8

8a. CONTRACT OR GRANT NO.
AF 19(628)-5167

b. PROJECT NO.
627A

c.
Purchase Order No. C-781

d.

9a. ORIGINATOR'S REPORT NUMBER(S)
2648-1

9b. OTHER REPORT NO(S) *(Any other numbers that may be assigned this report)*
ESD-TR-69-209

10. AVAILABILITY/LIMITATION NOTICES
This document has been approved for public release and sale; its distribution is unlimited.

11. SUPPLEMENTARY NOTES
None

12. SPONSORING MILITARY ACTIVITY
Air Force Systems Command, USAF

13. ABSTRACT

Dipole antennas with metallic shells for housing electronic equipment at the center which are called modified dipole antennas have been investigated. Measurements were made on the input admittances and far field patterns of the modified dipole antennas with cylindrical and spherical shells. The input admittances of 120° vee-antennas with spherical shells were also measured. The metallic shells were constructed in two diameters, 0.0625λ and 0.03125λ. The operating frequency used was 375 MHz.

Admittance measurements were made using a Hewlett-Packard Model 803A VHF Bridge. Input admittances were measured as a function of antenna wire length. Radiation patterns were measured in the $E_\Theta(\Theta)$ plane for various antenna wire lengths in the resonant region.

14. KEY WORDS

dipole antennas
antennas
electronic components
modified dipole antennas
communication satellites